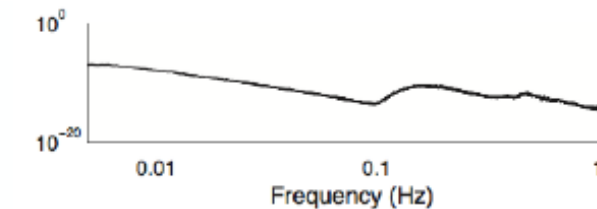
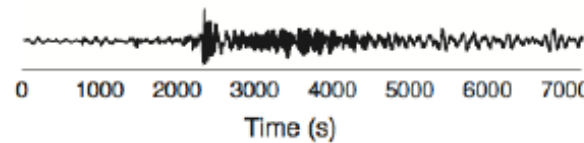


# Lecture 2: Seafloor noise and analyses

OBS training workshop, VUW, April 14-16, 2025

# Time series and spectra

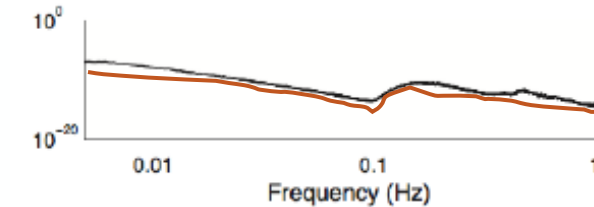
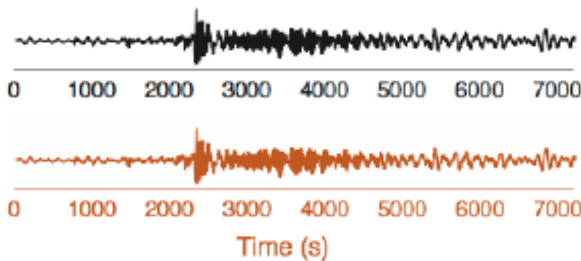


$$G_{xy}(f) = \frac{1}{n_d} \sum_{i=1}^{n_d} X_i^*(f) Y_i(f)$$

## Power Spectra

What is the power/amplitude of the time series at a given frequency?

# Time series and spectra



$$G_{xy}(f) = \frac{1}{n_d} \sum_{i=1}^{n_d} X_i^*(f) Y_i(f)$$

$$\gamma_{xy}^2(f) = \frac{|G_{xy}(f)|^2}{G_{xx}(f)G_{yy}(f)}$$

$$A_{xy}(f) = \frac{|G_{xy}(f)|}{G_{xx}(f)}$$

$$\phi_{xy}(f) = \arctan \left[ \frac{Q_{xy}(f)}{C_{xy}(f)} \right]$$

## Power Spectra

What is the power/amplitude of the time series at a given frequency?

## Coherence

At a given frequency, how “coherent” are two signals? How much of y can I predict, if I know x?

## Admittance

Gain factor of the *transfer function*. If I want to relate the x and y components, what constant do I multiply as a function of frequency?

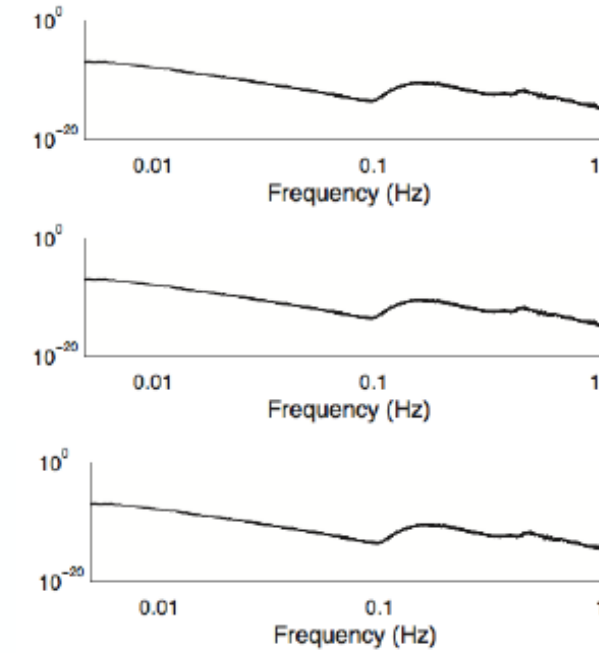
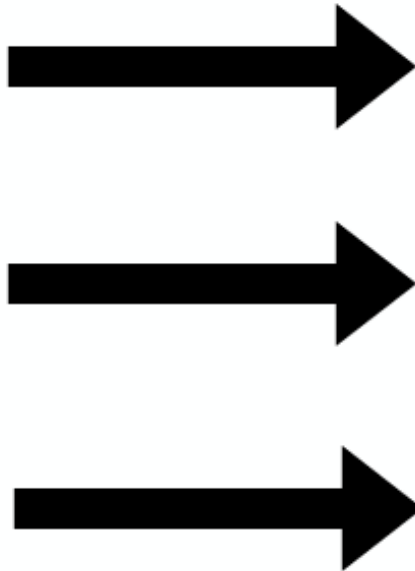
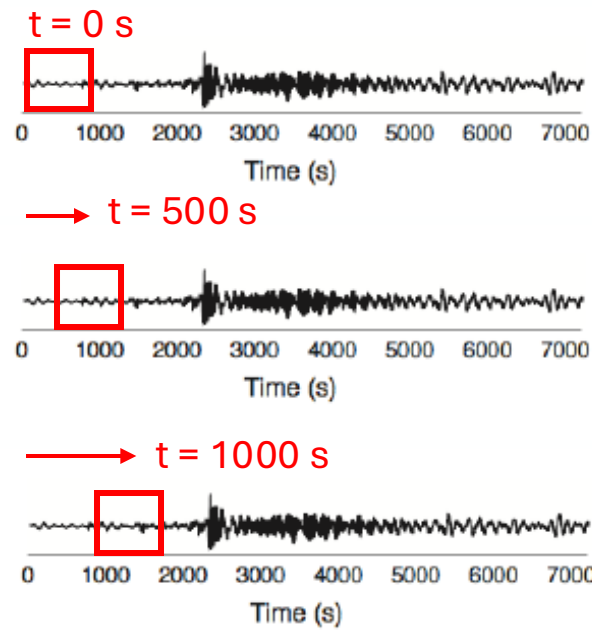
## Phase

If the signals are coherent, what’s the cycle separation between x and y?

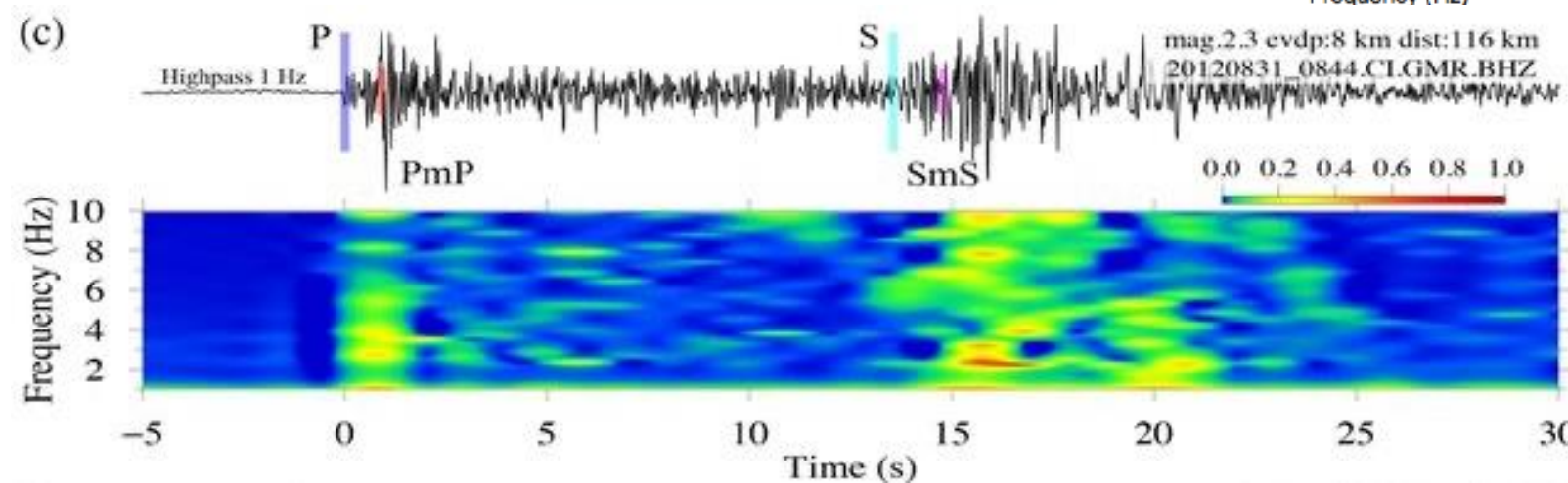
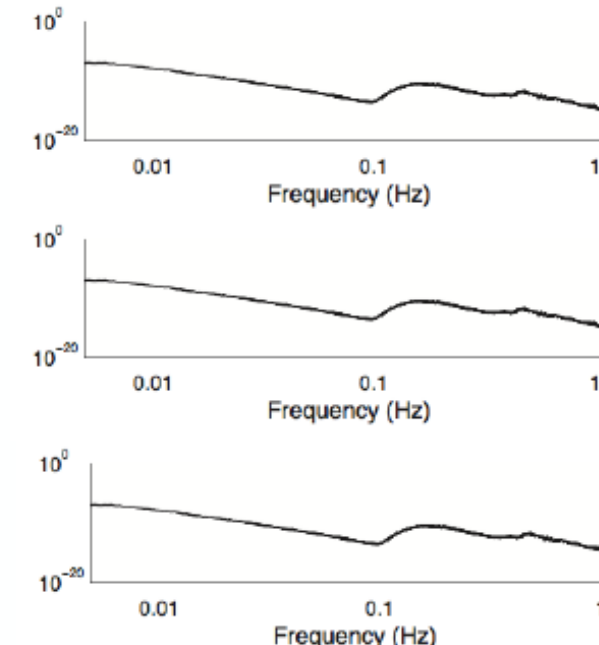
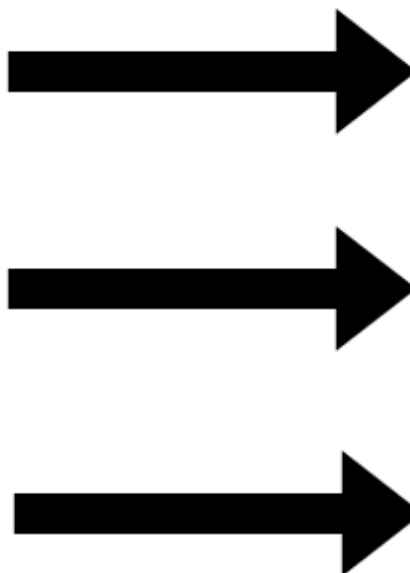
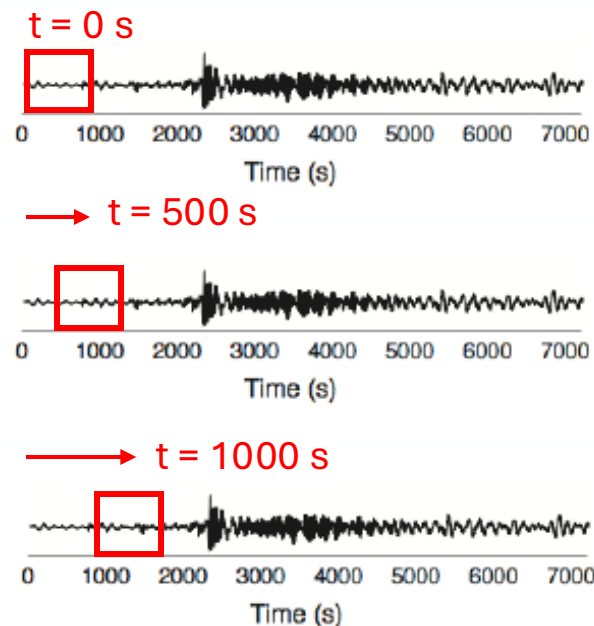
# Spectrogram

- A spectrogram is a visual representation of the spectrum of frequencies of a signal as it varies with time.
- A digitally sampled signal in the time domain is divided into (overlapping) chunks and Fourier-transformed to calculate the frequency spectrum's magnitude for each chunk.
- Instead of averaging, each chunk corresponds to a vertical line in the image, i.e., a measurement of magnitude versus frequency for a specific moment in time (the start or midpoint of the chunk).
- These spectra or time plots are then "laid side by side" to form the image or a three-dimensional surface.

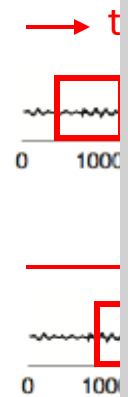
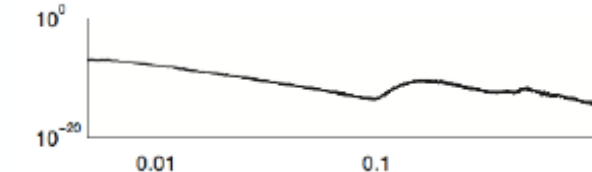
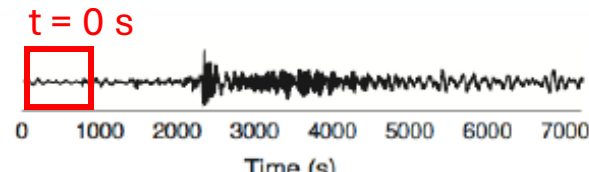
# Spectrogram



# Spectrogram

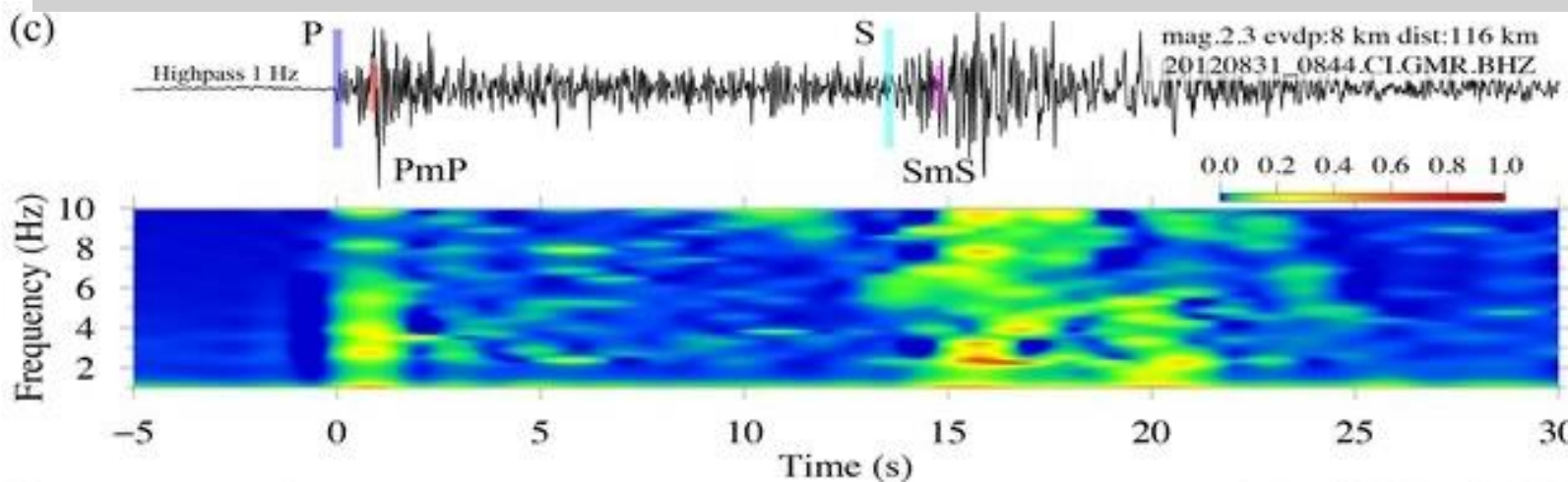


# Spectrogram



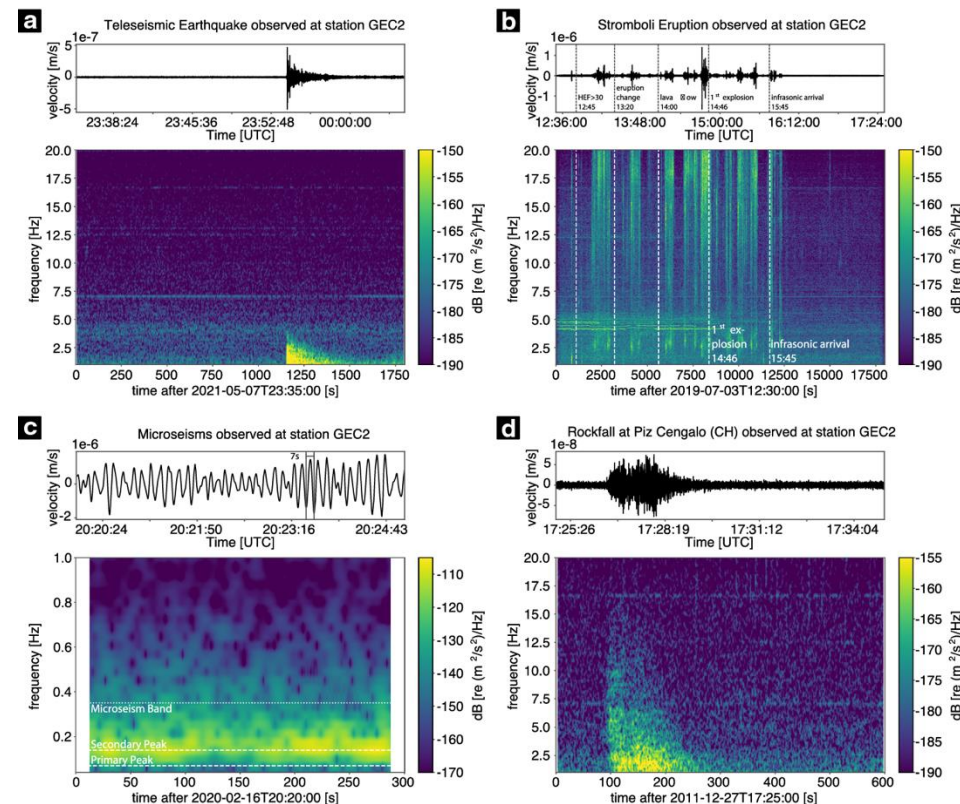
- Vertical band in spectrogram: Spike in energy (i.e., body-wave phase arrival)
- Horizontal band in spectrogram: Harmonic signal

(c)



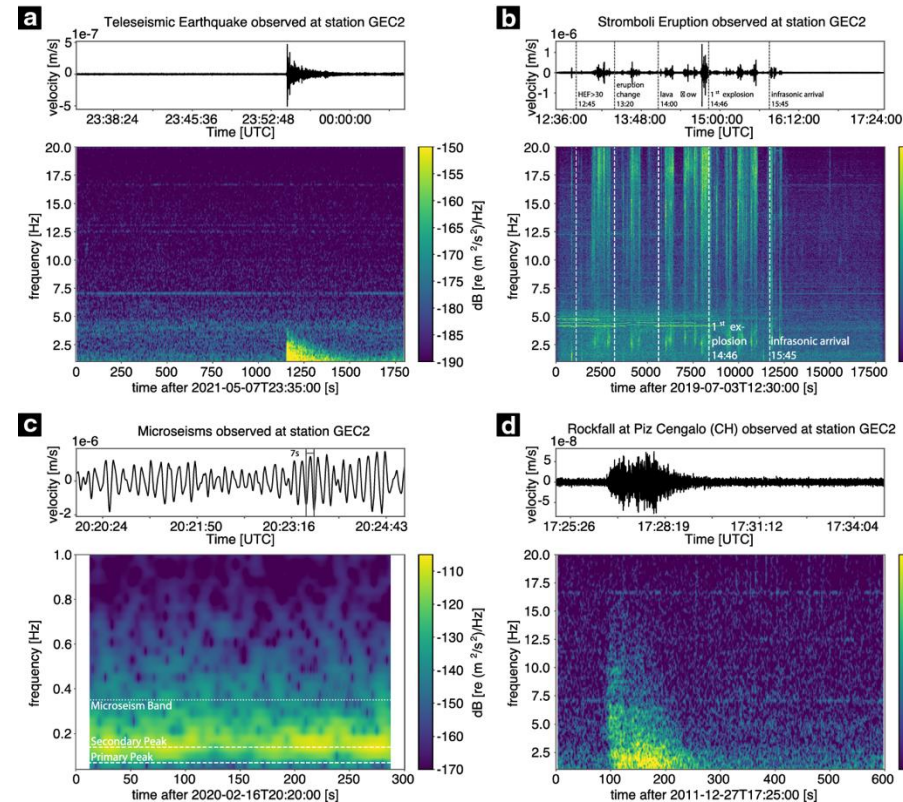
# Spectrograms of seismic/hydroacoustic signals

## Seismic signals

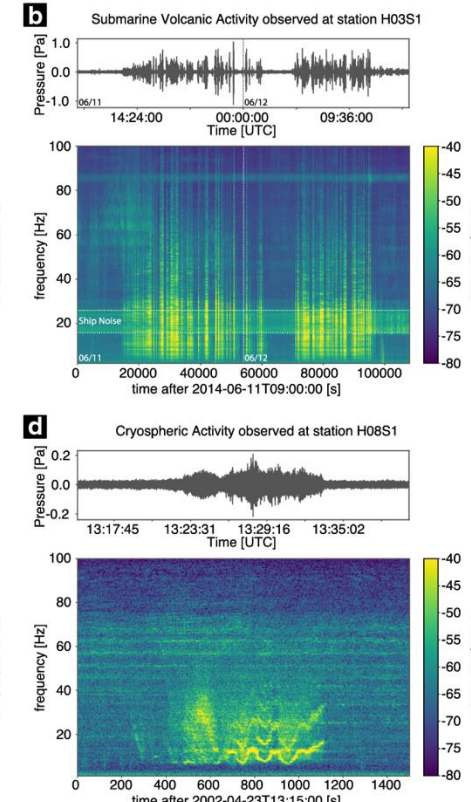


# Spectrograms of seismic/hydroacoustic signals

## Seismic signals

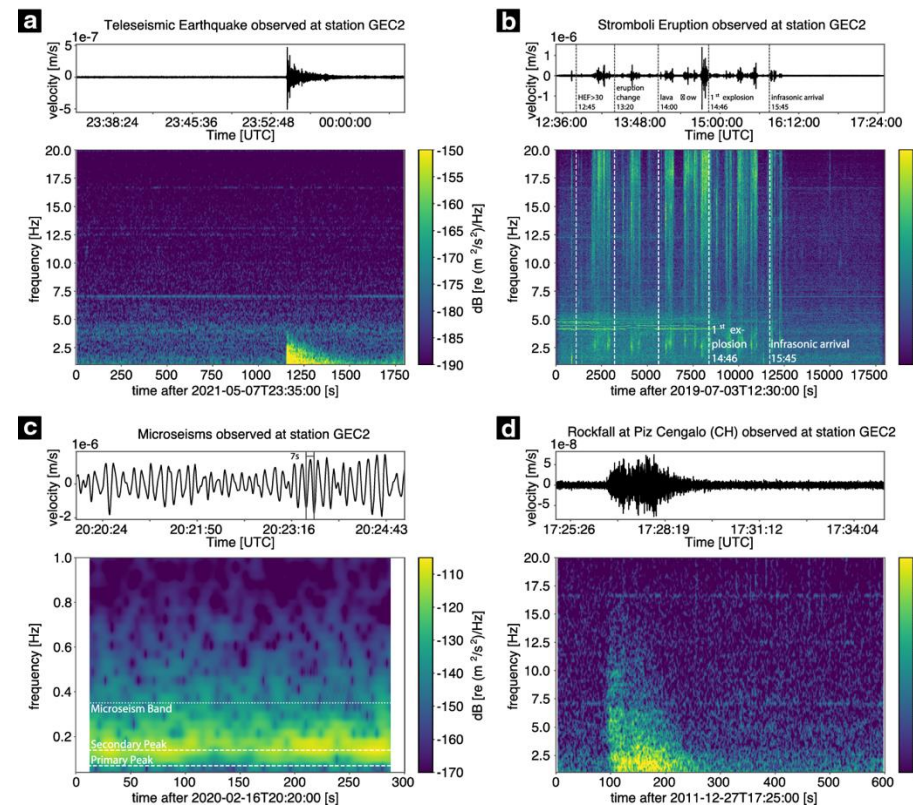


## Hydroacoustic signals

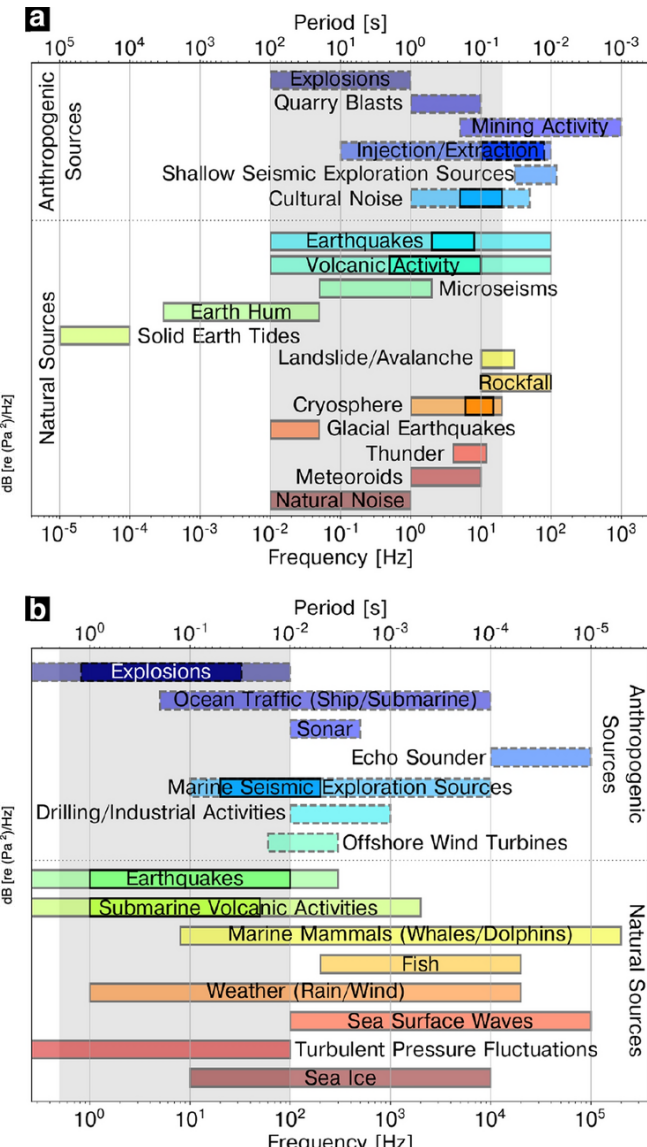
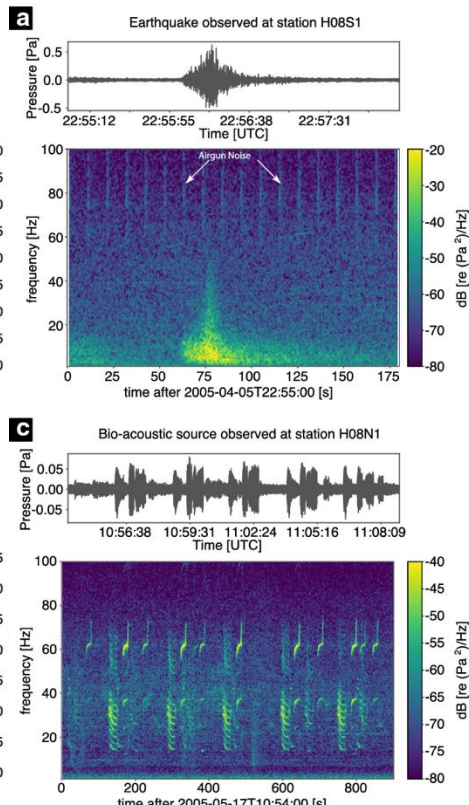


# Spectrograms of seismic/hydroacoustic signals

## Seismic signals

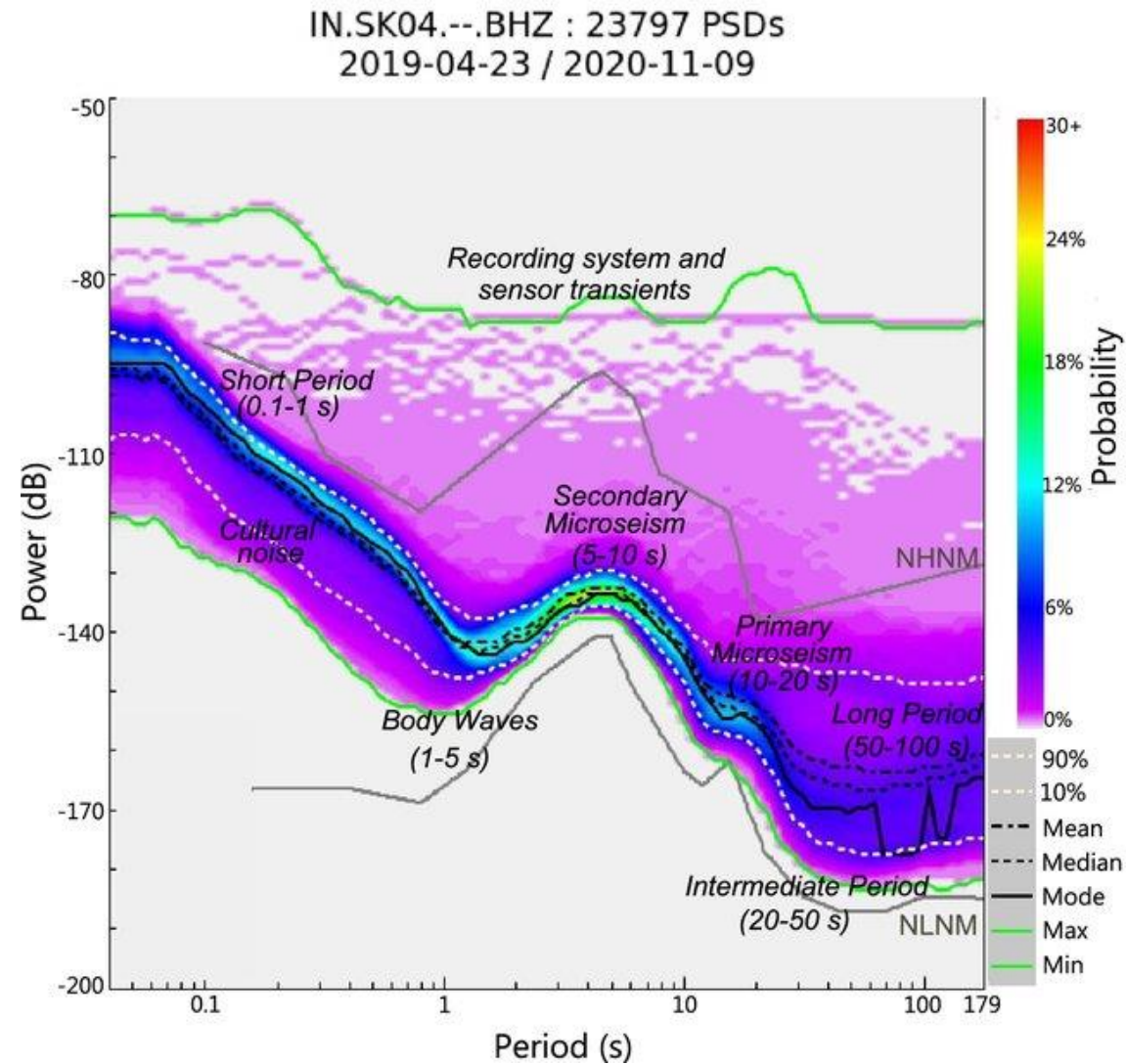


## Hydroacoustic signals



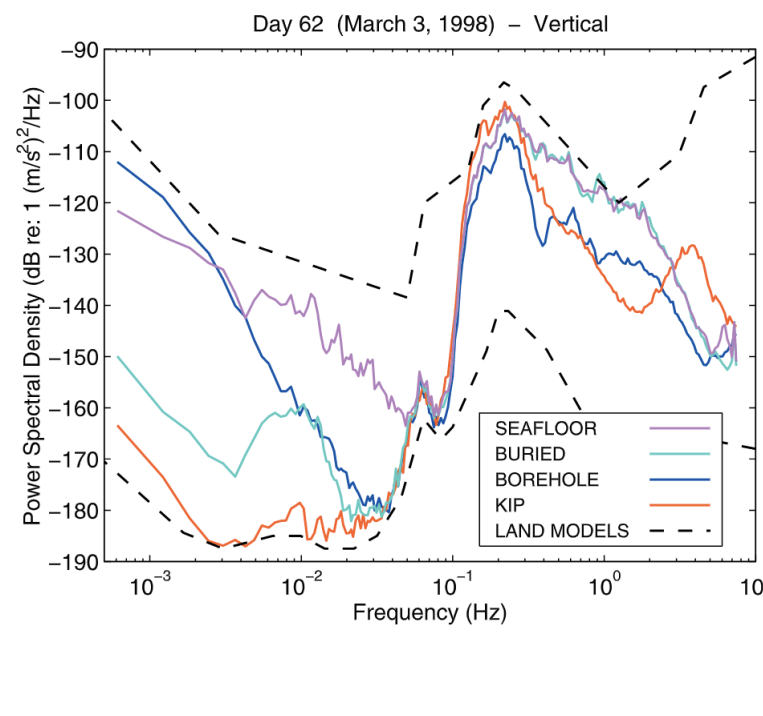
# Seismic noise basics

- Seismic ambient noise is the result of several « forcings » in the Earth
  - Earth's « hum » (30-300 s)
  - Primary microseismic peak (10-20 s)
  - Secondary microseismic peak (5-10 s)
  - Cultural noise (< 1 s)
- Natural forcings are due to:
  - Ocean waves and gravity waves
  - Wind and atmospheric disturbances
  - Local site conditions

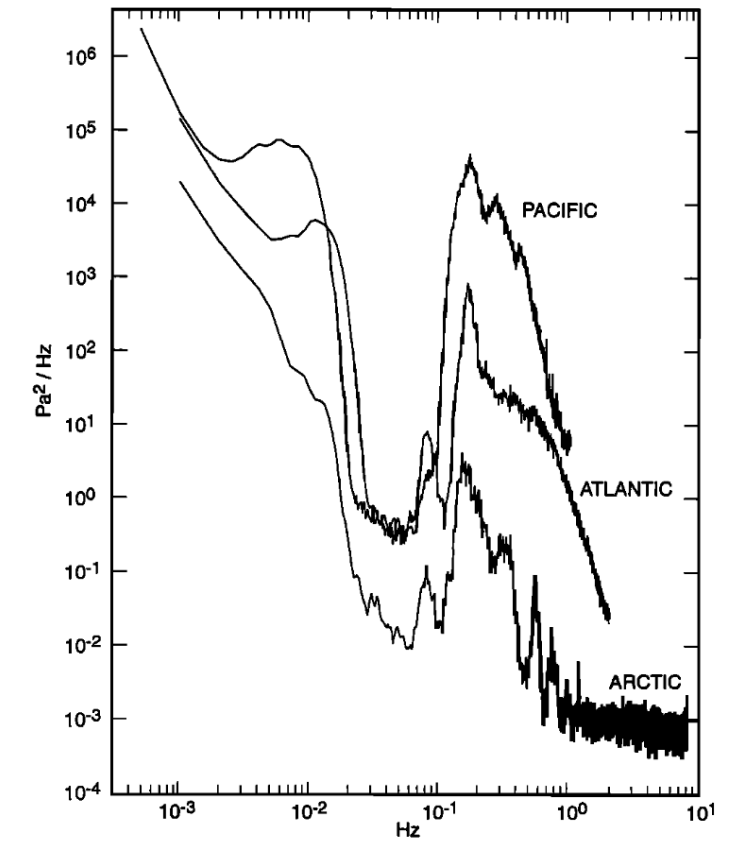


# OBS noise basics

- OBS data are NOISY! OBS noise characteristics depend on MANY factors, including:
  - Station and network design
  - Deployment depth
  - Ocean noise properties
  - Seafloor coupling, etc.

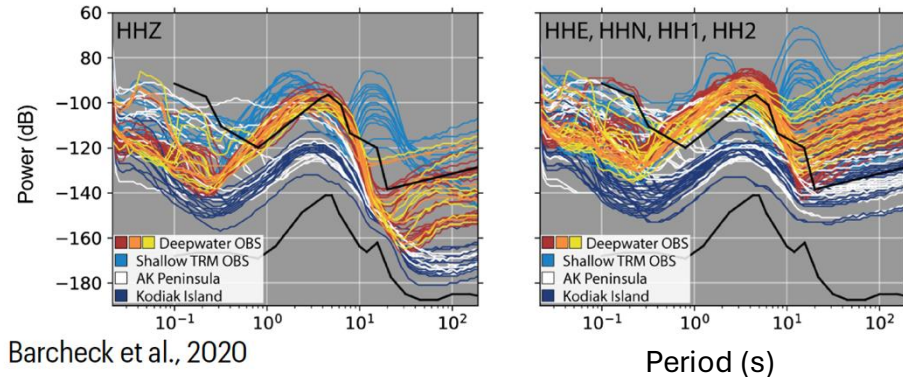


Stephen et al. (2002)



Webb (1998)

# OBS noise basics

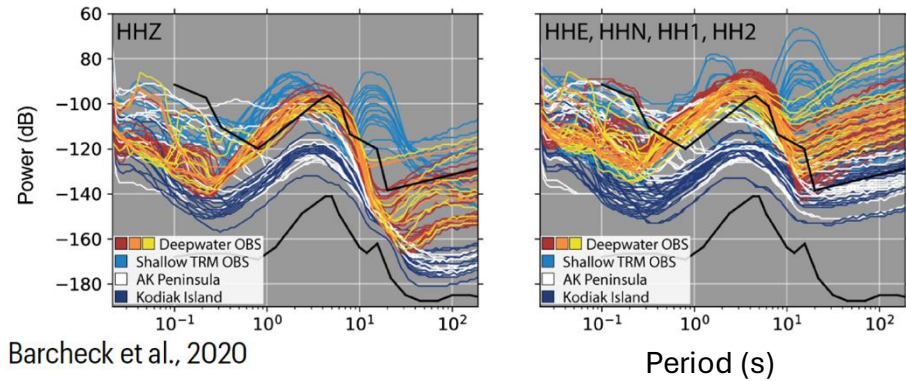


Barchek et al., 2020

OBS data are relatively noisy, in part due to  
**compliance** and **tilt** noise.

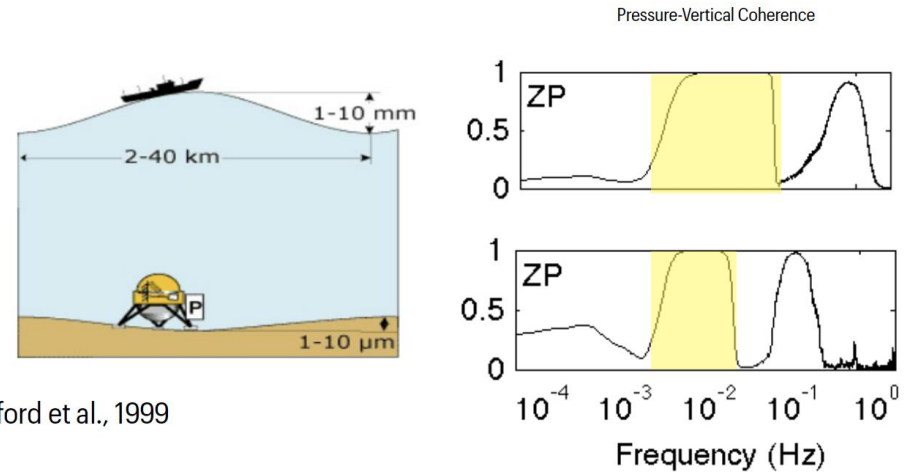
- Greater long-period noise compared to land station
- Greater noise for shallow OBS (notice additional peak)
- Much greater noise on horizontal component.

# OBS noise basics



Barchek et al., 2020

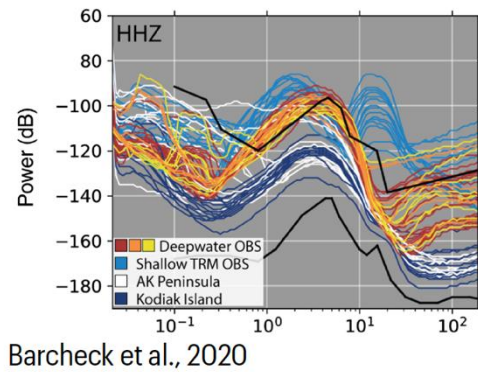
OBS data are relatively noisy, in part due to **compliance** and **tilt** noise.



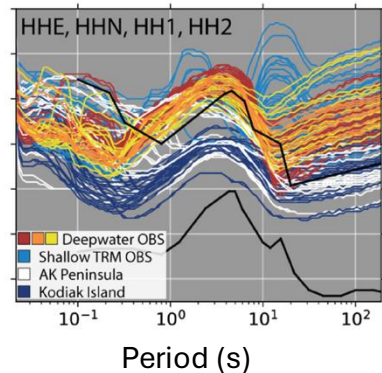
Crawford et al., 1999

Infragravity waves induce **compliance** noise, which has a frequency-depth dependence.

# OBS noise basics

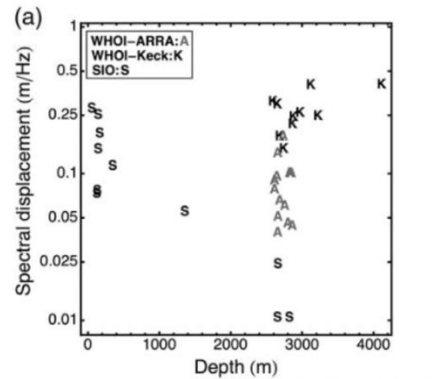
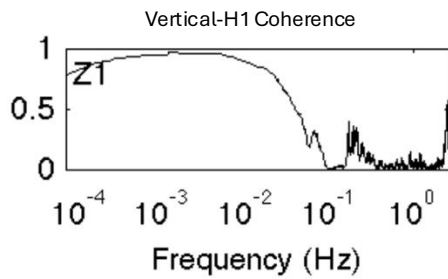


Barchek et al., 2020



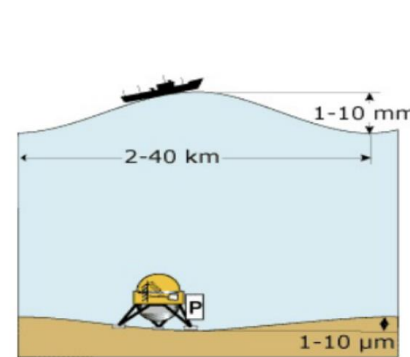
Period (s)

OBS data are relatively noisy, in part due to **compliance** and **tilt** noise.

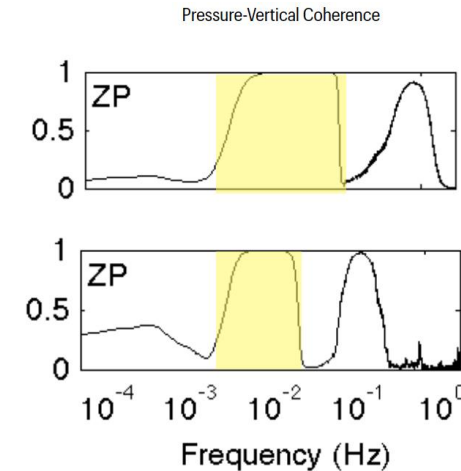


Bell et al., 2015

Bottom currents cause **tilt** noise, which may vary with instrument design.



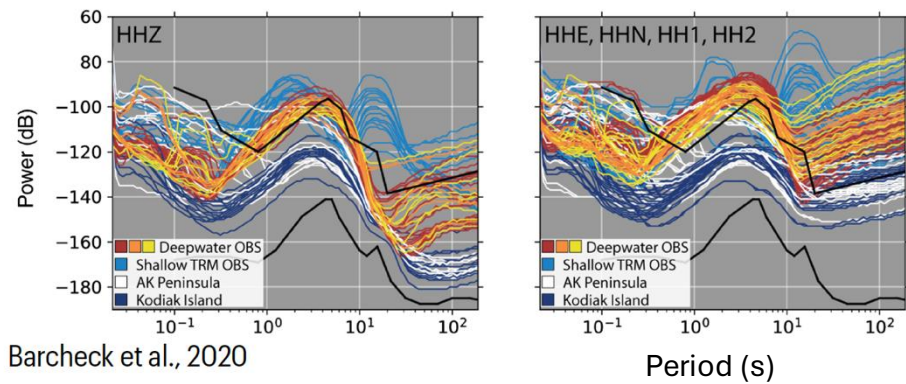
Crawford et al., 1999



Pressure-Vertical Coherence

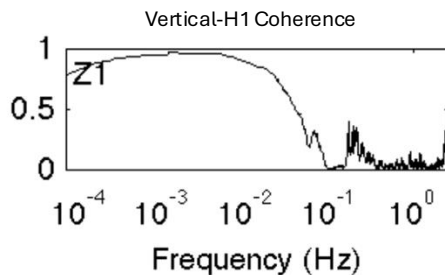
Infragravity waves induce **compliance** noise, which has a frequency-depth dependence.

# OBS noise basics

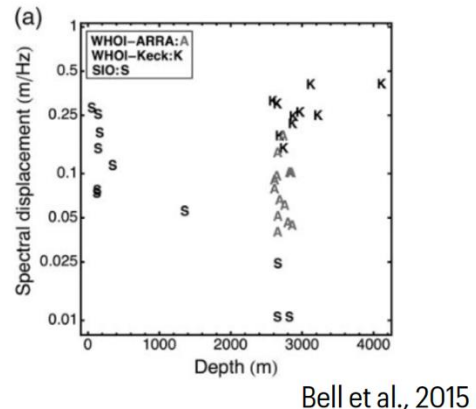


Barchek et al., 2020

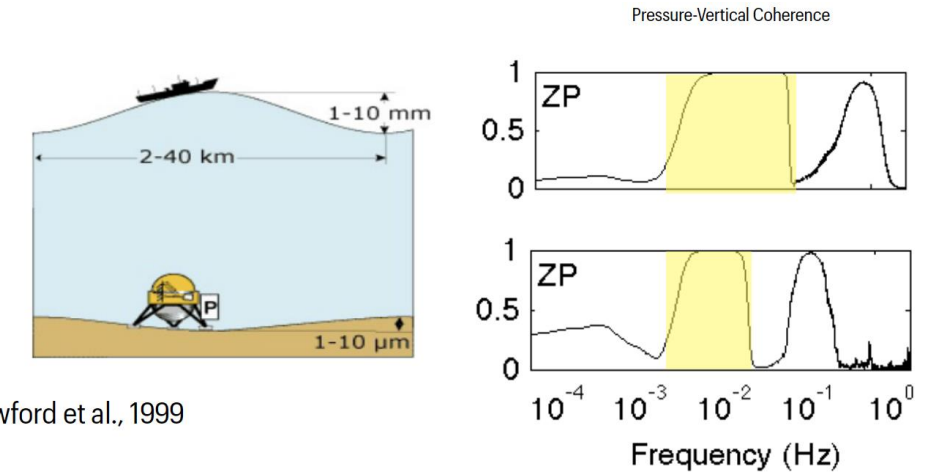
OBS data are relatively noisy, in part due to **compliance** and **tilt** noise.



Bottom currents cause **tilt** noise, which may vary with instrument design.

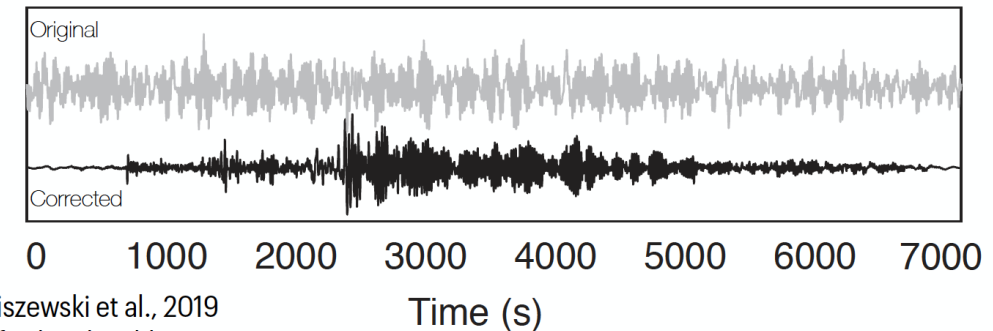


Bell et al., 2015



Crawford et al., 1999

Infragravity waves induce **compliance** noise, which has a frequency-depth dependence.



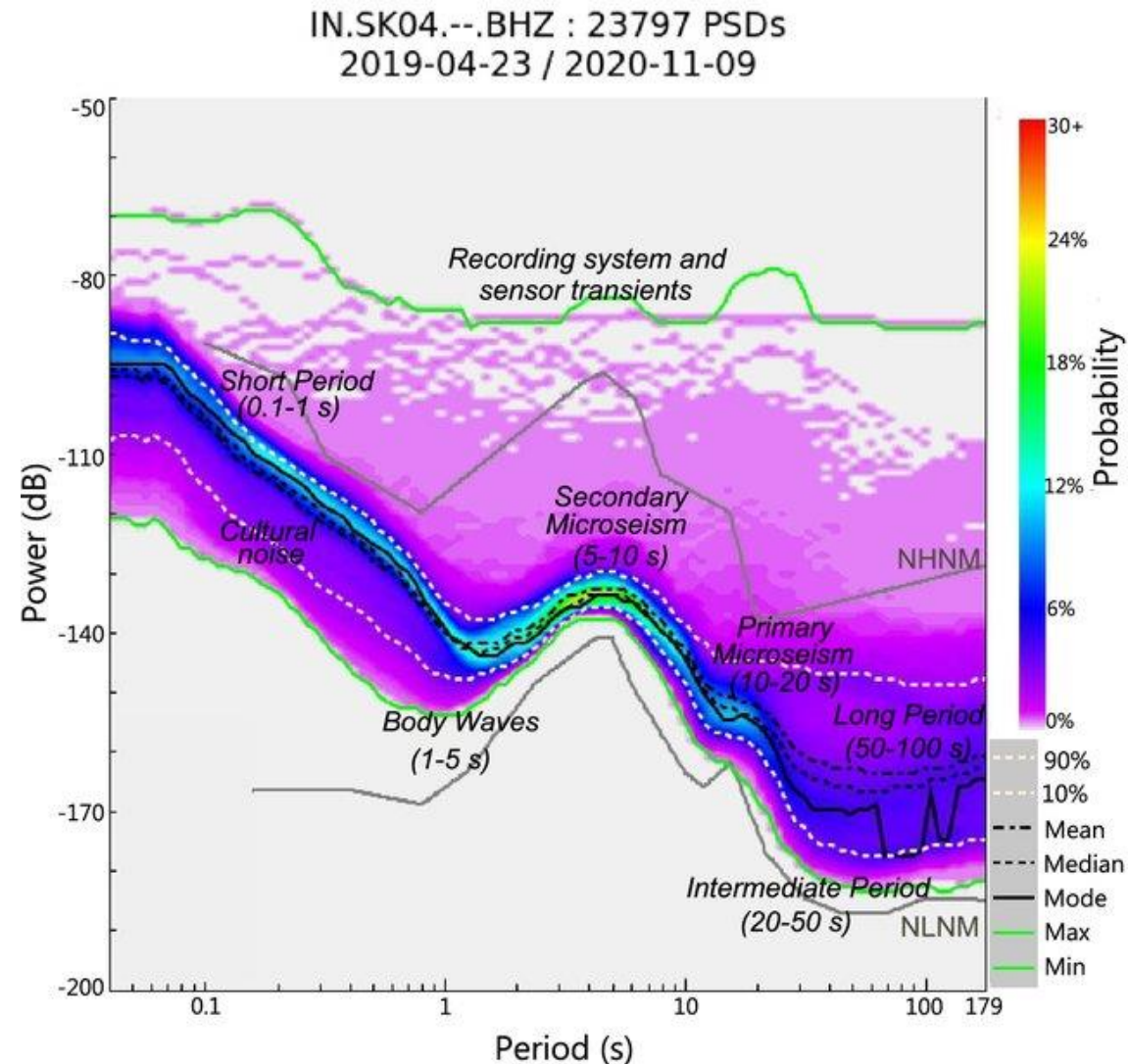
Janiszewski et al., 2019  
Crawford and Webb, 2000

**Tilt** and **compliance** noise can be removed from vertical components, improving data quality.

**Tutorial 3: Compliance + tilt corrections**

# What works where and why?

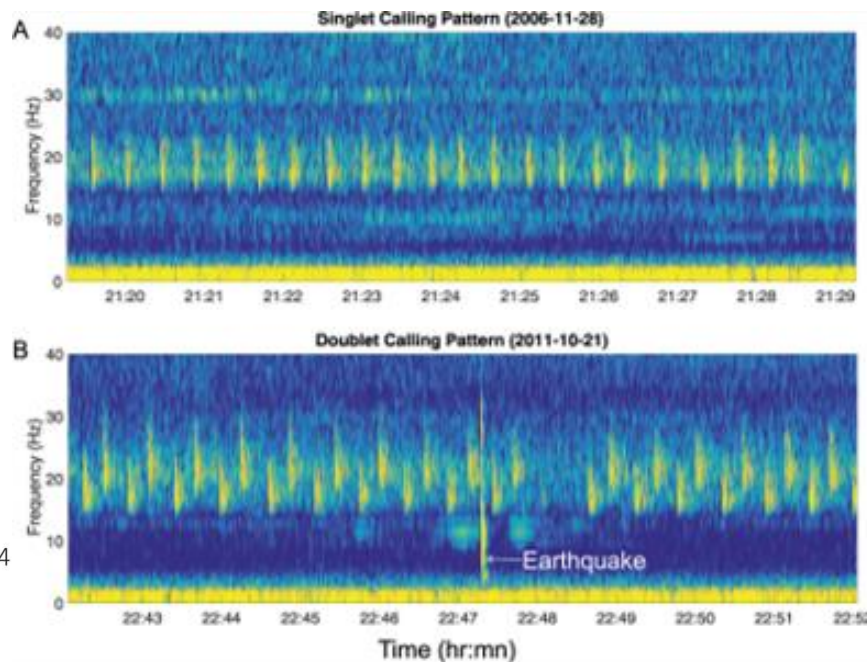
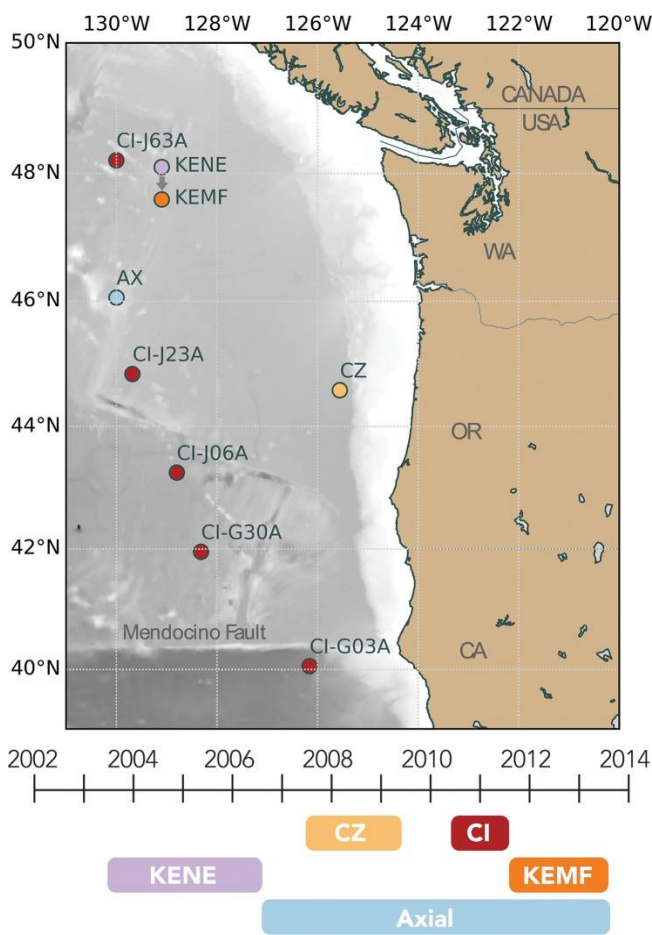
- The feasibility of any seismological technique depends on the level of noise at the frequency of interest:
  - **Body waves:** teleseismic (0.1-1 Hz), regional (0.5-5 Hz), local (5-20 Hz)
  - **Surface waves:** noise interferometry (5-30 sec), regional (10-80 sec), teleseismic (20-200 sec)
- How can you properly estimate potential noise levels (and the viability of certain techniques) when planning your deployment?
- How can you quickly assess if a method is likely to work with your data once you have collected your instruments?



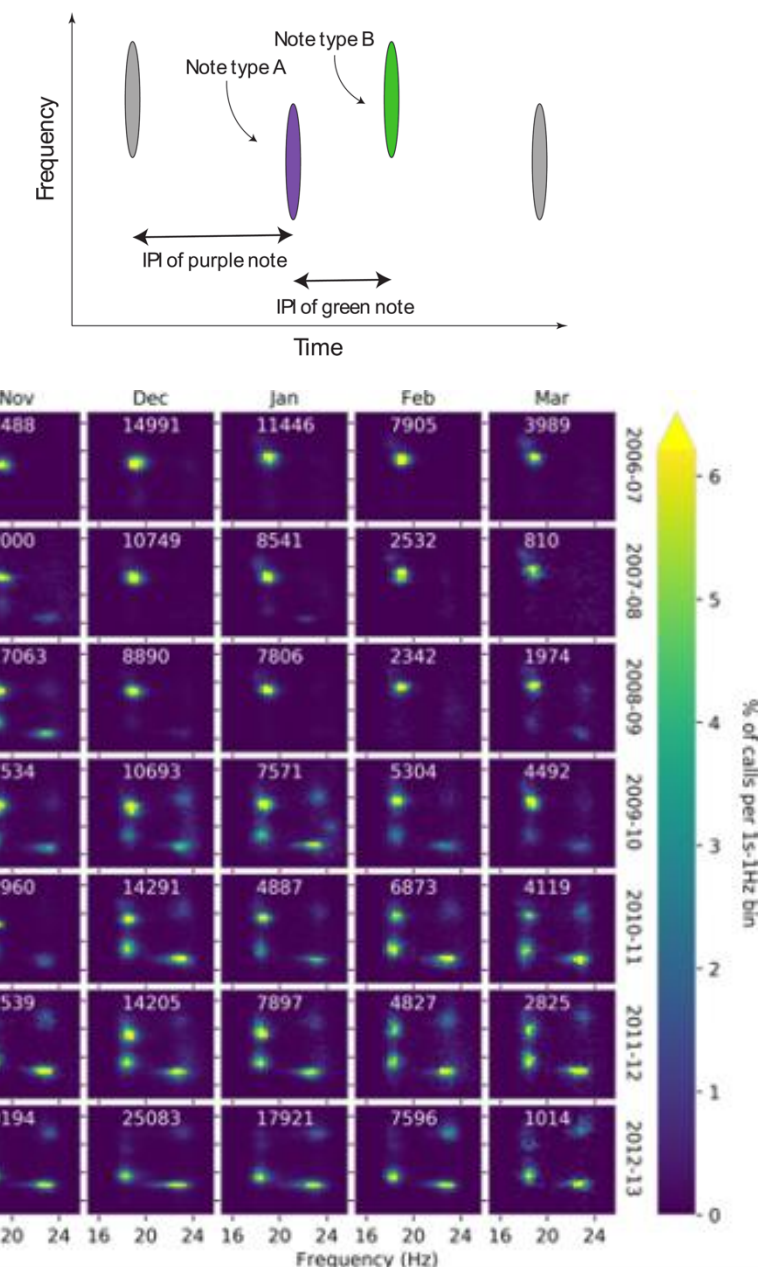
# Non-earthquake signals in the ocean

- Just as land seismometers can pick up a variety of sources that produce ground shaking (e.g., traffic, storms, wildlife), OBS stations record unusual signals.
- Examples include whale vocalizations, turbidity currents, ice calving, volcanic eruptions, nuclear tests/explosions, ships, etc.

# Tracking whales with OBS



Fin whale 20-Hz vocalizations recorded by OBS showing two call patterns: single-frequency single inter-pulse interval; doublet pattern --> help determine population distributions  
<https://www.youtube.com/watch?v=gUfHvz-MRIs>

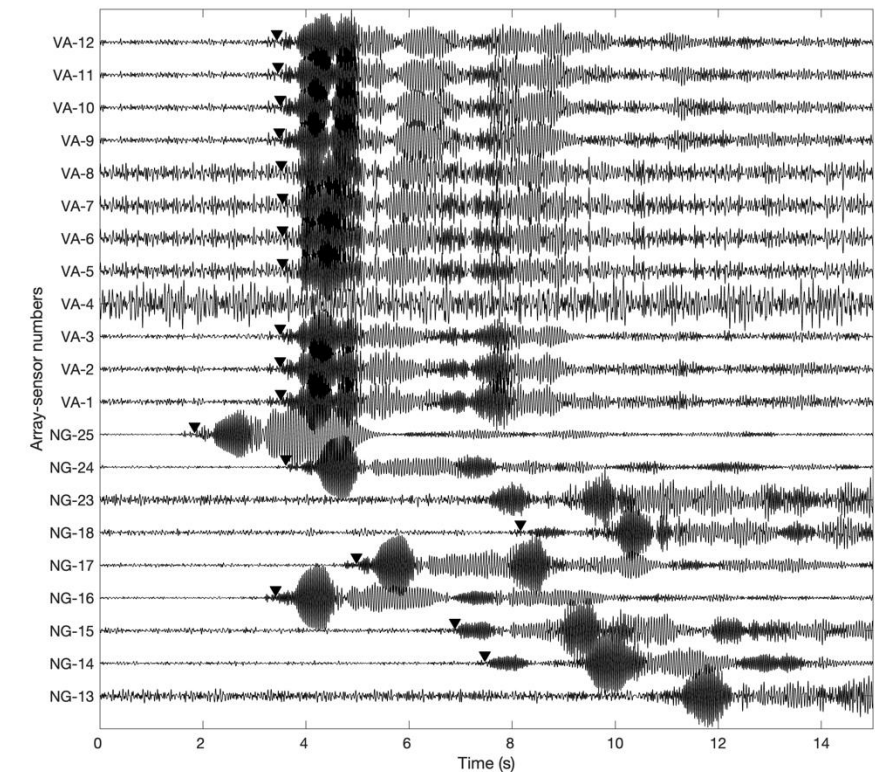
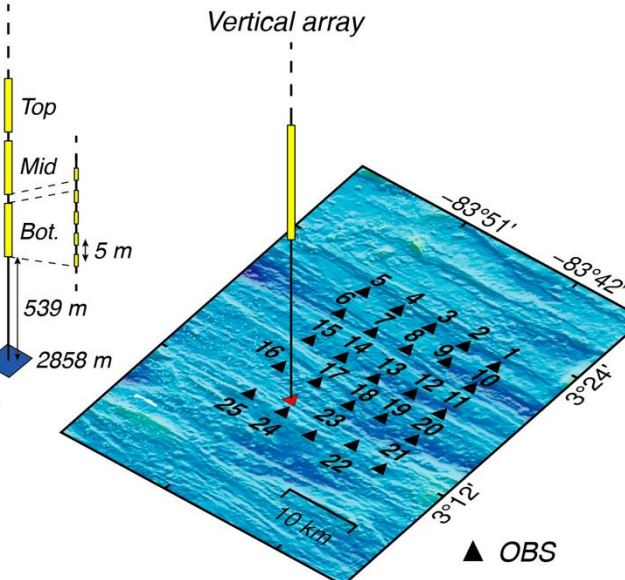
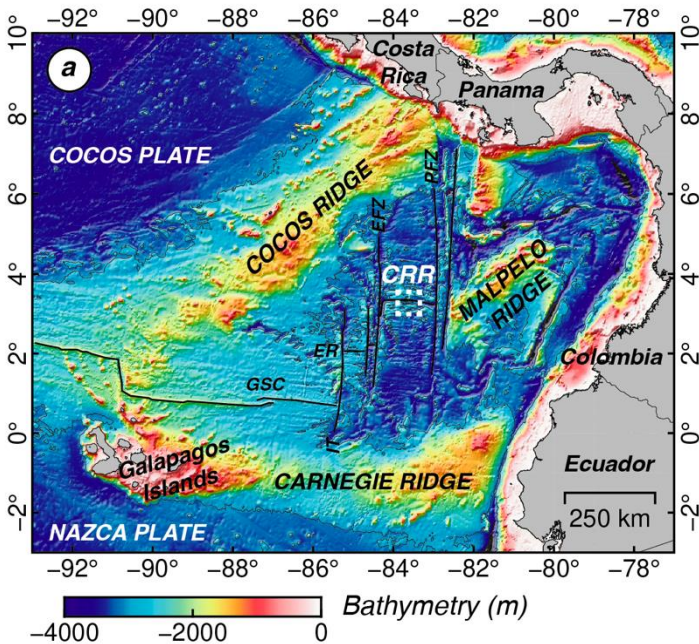


Weirathmueller et al. (2017)

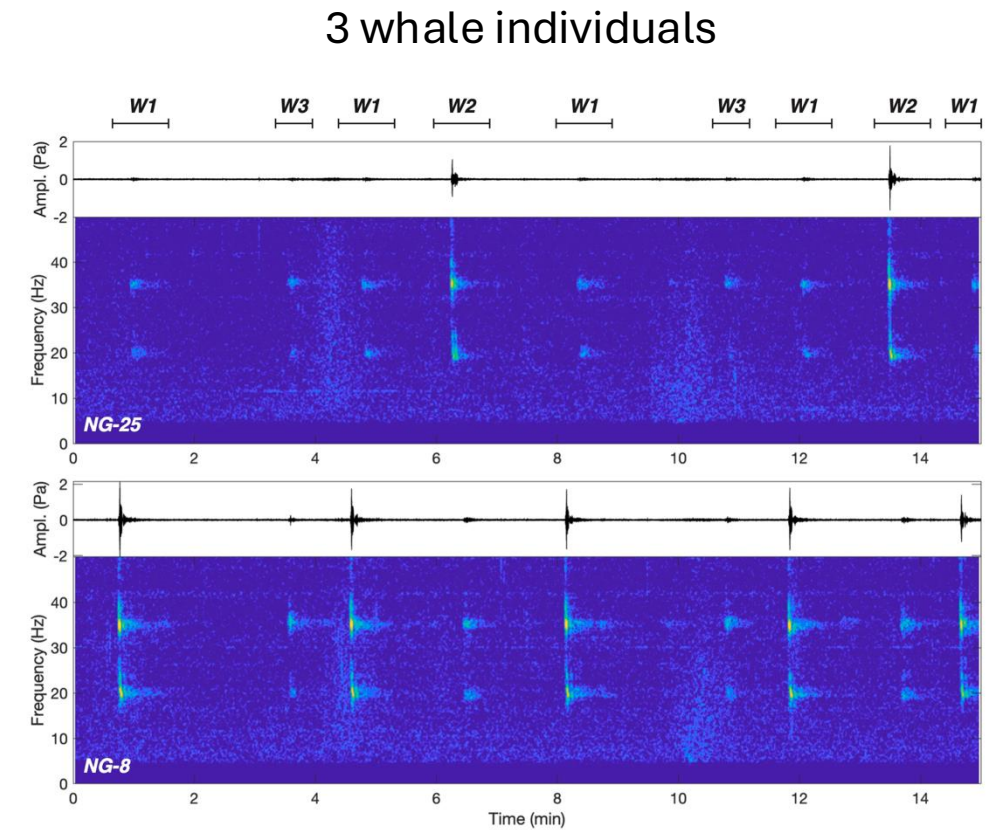
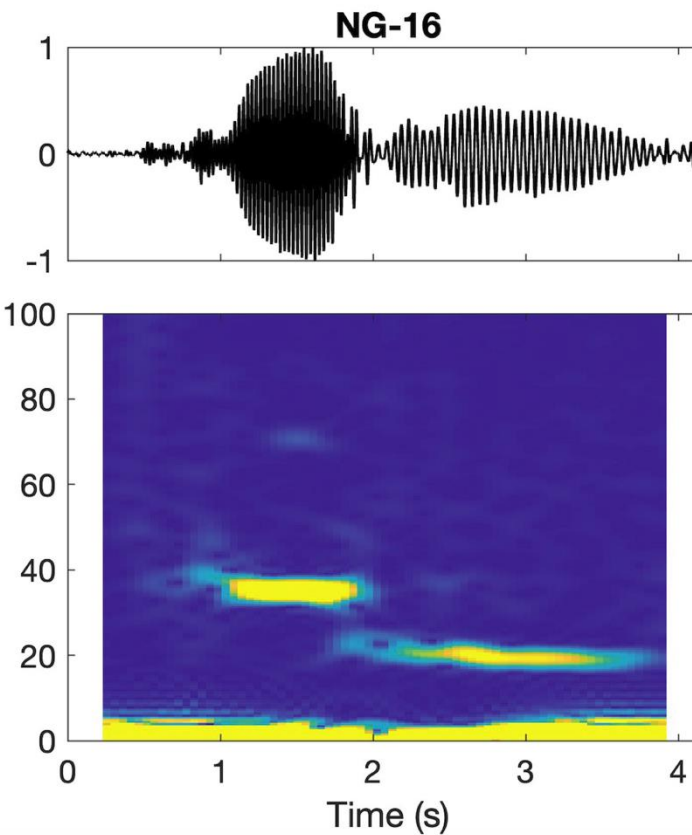
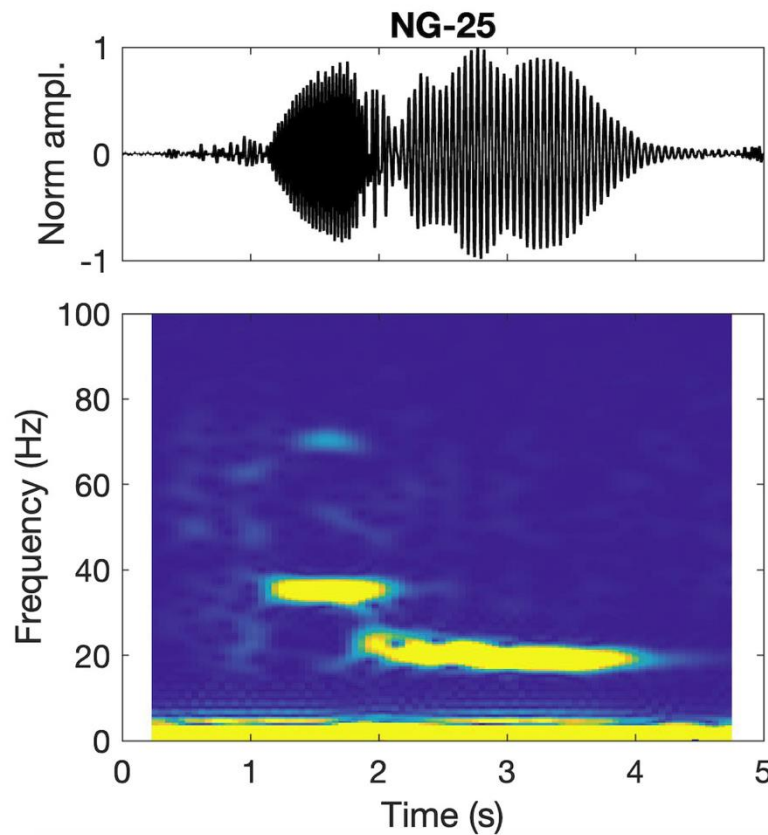
# Tacking whale calls

Application of a seismic network to baleen whale call detection and localization in the Panama basin – a Bryde's whale example

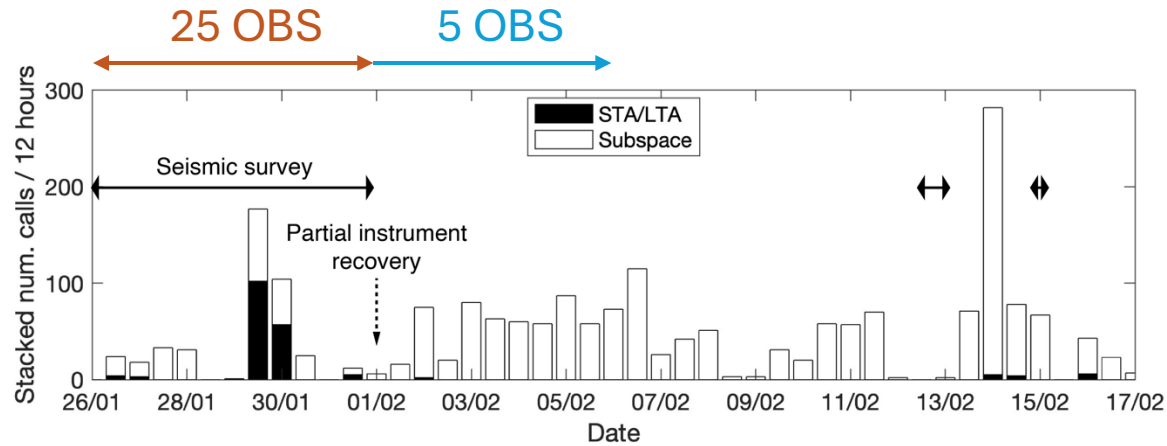
Jean Baptiste Tary<sup>1,2</sup>, Christine Peirce<sup>3</sup>, Richard W. Hobbs<sup>3</sup>, Felipe Bonilla Walker<sup>1</sup>, Camilo De La Hoz<sup>1,4</sup>, Anna Bird<sup>3</sup>, and Carlos Alberto Vargas<sup>5</sup>



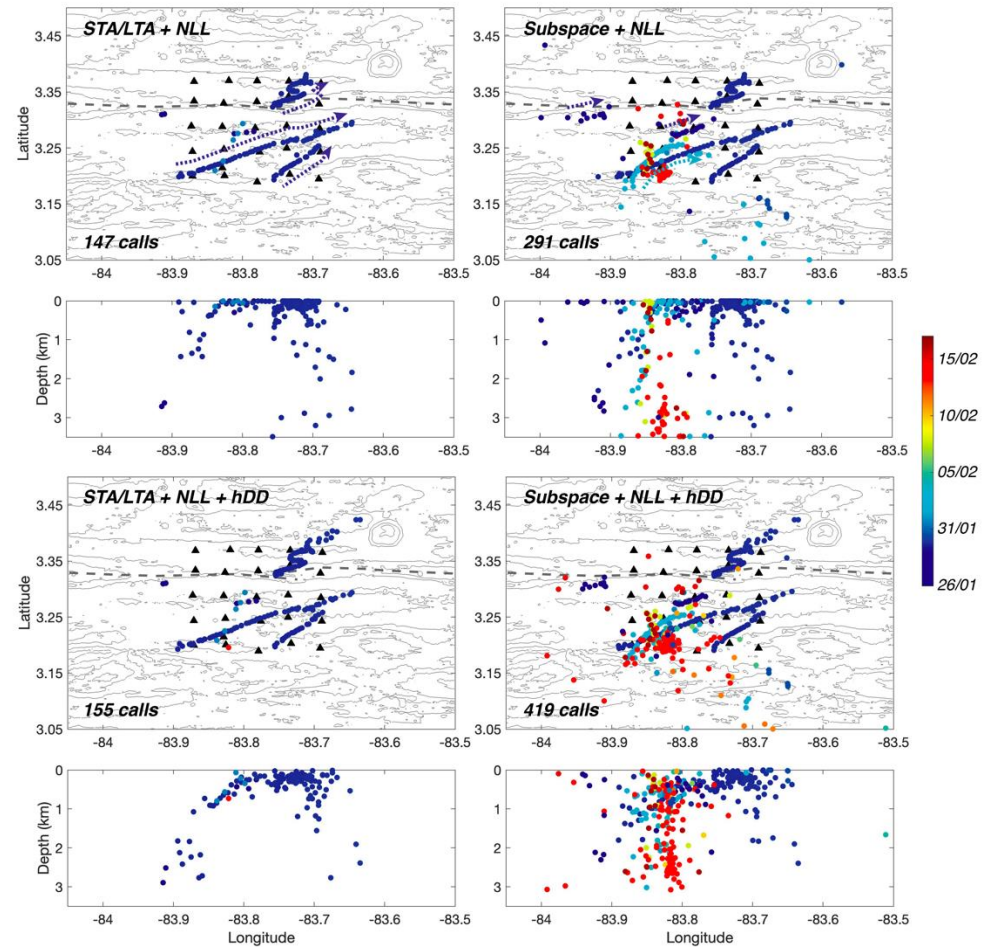
# Whale call signatures: Bryde's whales



# Whale call detection and location



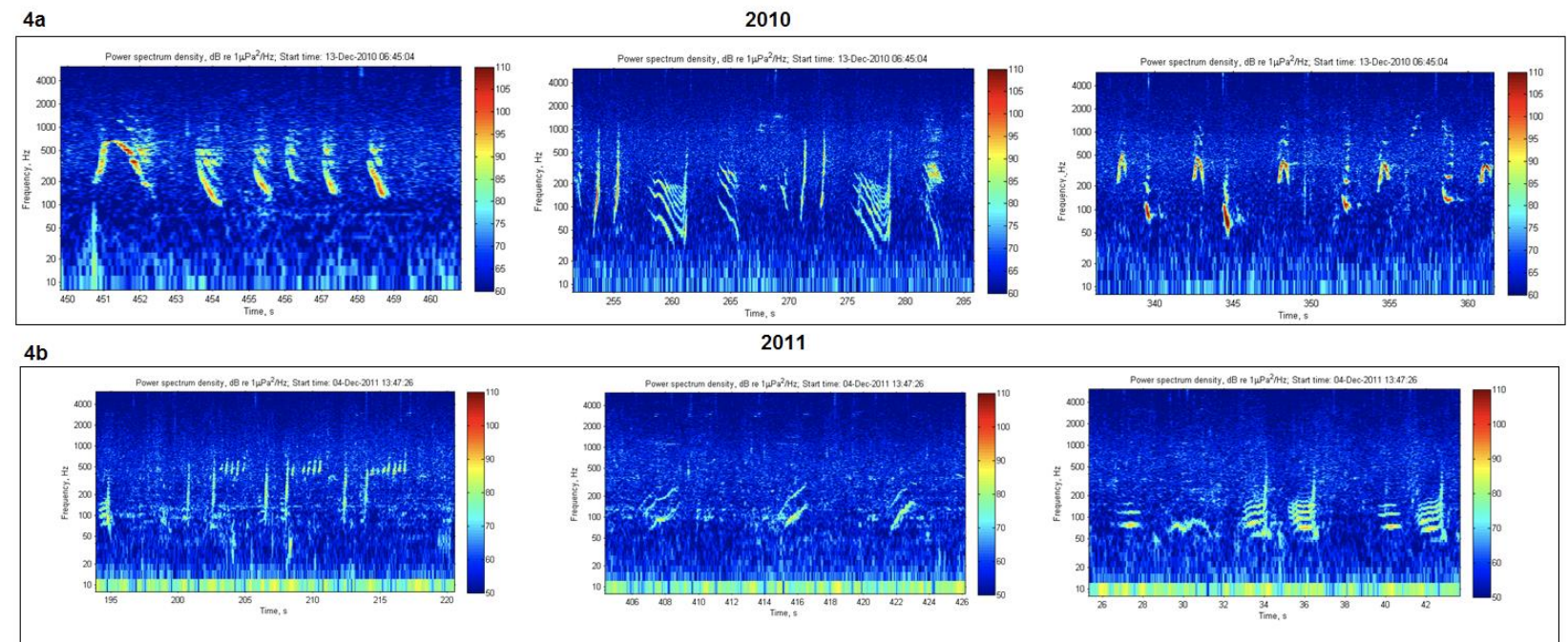
- Temporal distribution of whale call number detected using the STA/LTA (black bars) and network empirical subspace detector (white bars) for OBS + hydrophones.
- Whale call localizations, laterally and with depth, for the events detected using the STA/LTA and the empirical subspace detector, and localized using NonLinLoc (NLL) and hypoDD (hDD). Only events with horizontal uncertainties lower than  $\pm 5$  km are shown.



# Humpback whales and ELVES



- Northward migration along the coast June – August
- Vocalizations are high-frequency: 50 to >500 Hz
- May be picked up by Aquarius seismometers (sampling rate of 250 Hz)

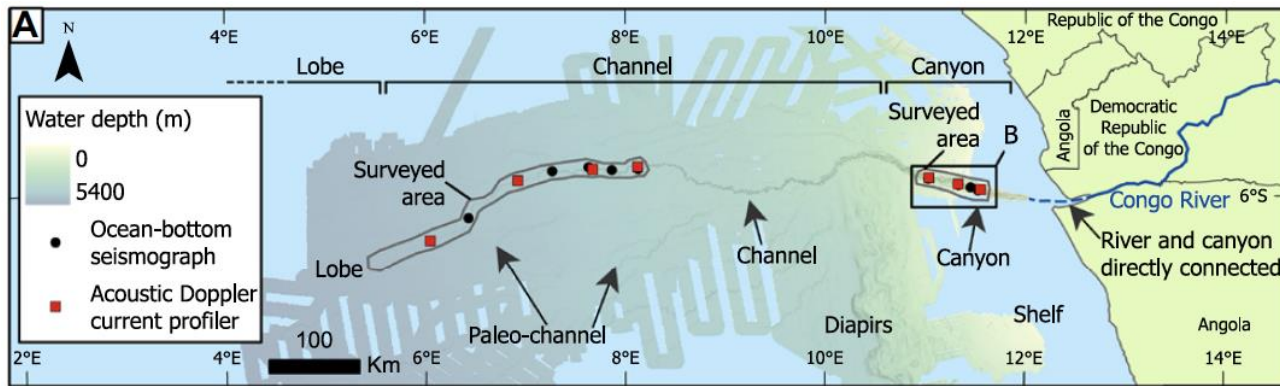


# Tracking turbidity currents

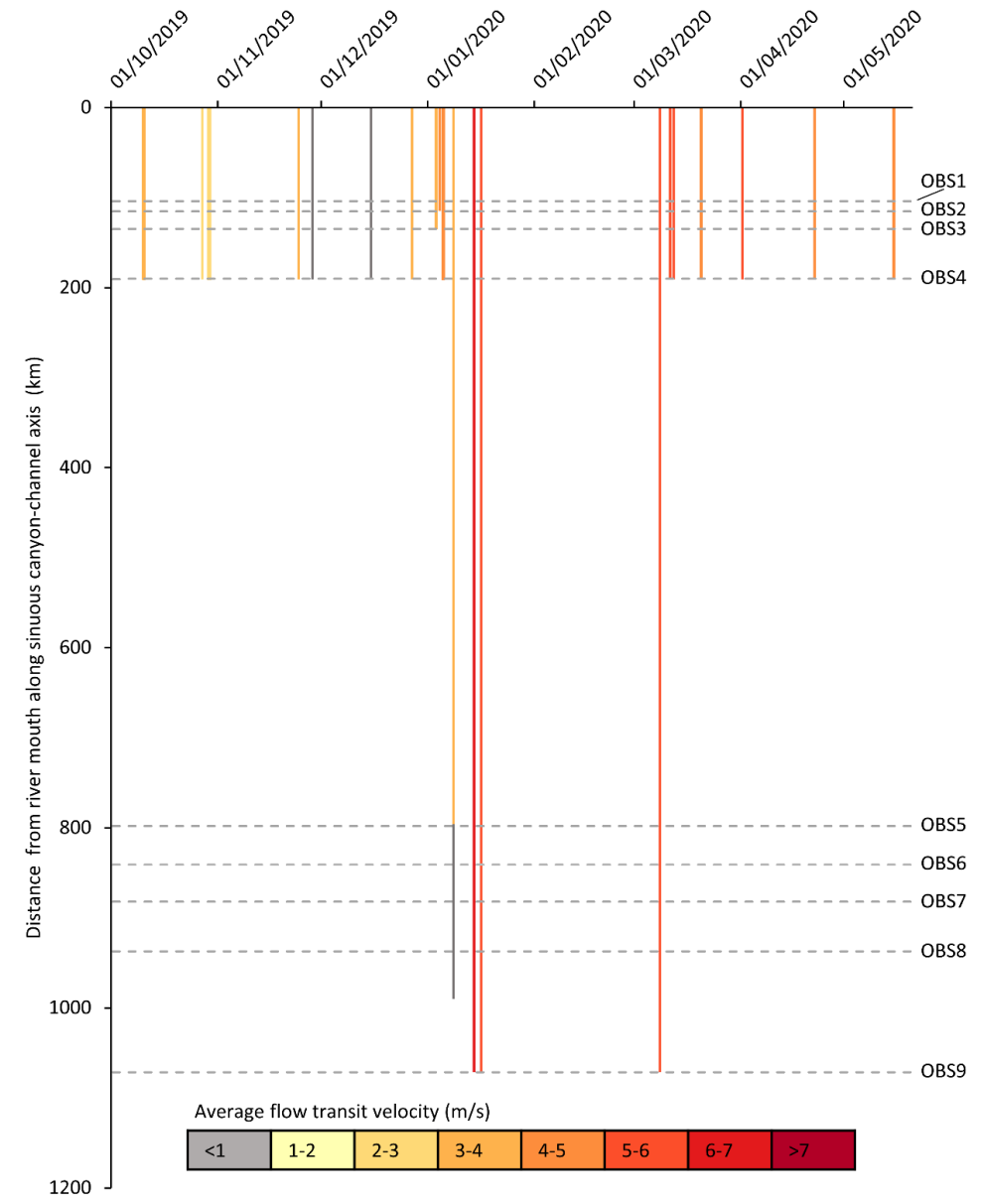
Globally significant mass of terrestrial organic carbon efficiently transported by canyon-flushing turbidity currents

Megan L. Baker<sup>1,\*</sup>, Sophie Hage<sup>2</sup>, Peter J. Talling<sup>1,3</sup>, Sanem Acikalin<sup>4</sup>, Robert G. Hilton<sup>5</sup>, Negar Haghipour<sup>6,7</sup>, Sean C. Ruffell<sup>8</sup>, Ed L. Pope<sup>1</sup>, Ricardo Silva Jacinto<sup>2</sup>, Michael A. Clare<sup>8</sup>, and Sefa Sahin<sup>4</sup>

- Submarine turbidity currents are volumetrically the most important sediment transport processes on Earth, yet poorly understood and documented.

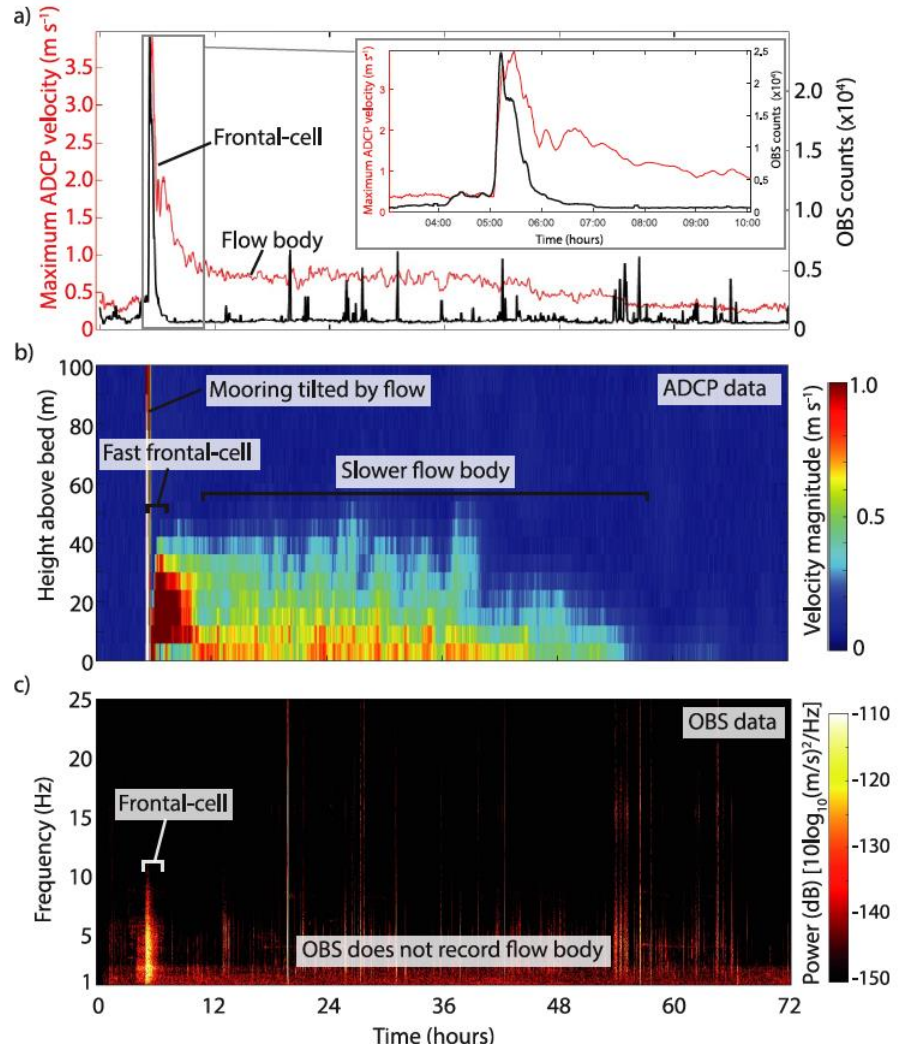


- OBS data was processed to reveal the timing of turbidity currents.
- The only information used is the onset of increased ground shaking on the vertical component.

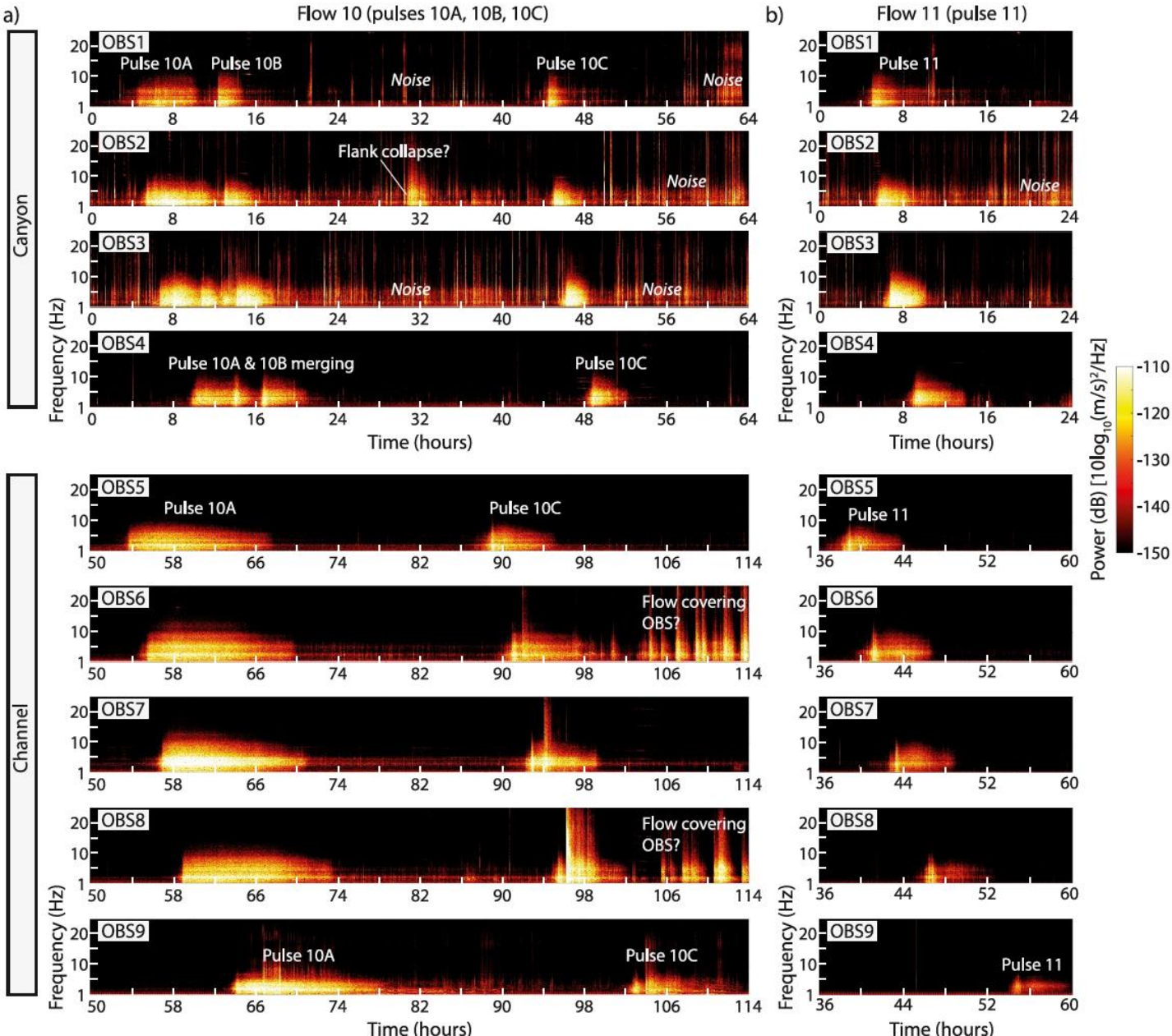


# Seabed Seismographs Reveal Duration and Structure of Longest Runout Sediment Flows on Earth

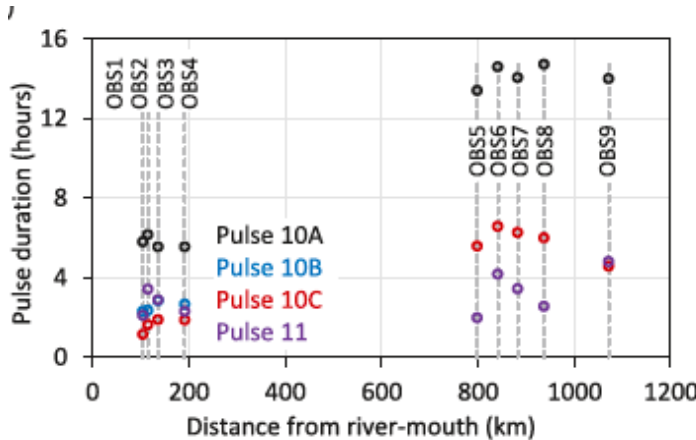
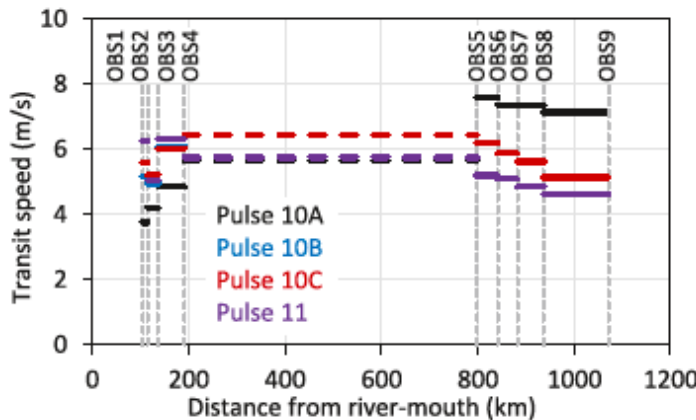
Megan L. Baker<sup>1</sup> , Peter J. Talling<sup>1,2</sup> , Richard Burnett<sup>3</sup>, Ed L. Pope<sup>1</sup> , Sean C. Ruffell<sup>2</sup> , Morelia Urlaub<sup>4</sup> , Michael A. Clare<sup>5</sup>, Jennifer Jenkins<sup>2</sup> , Michael Dietze<sup>6,7</sup> , Jeffrey Neasham<sup>3</sup> , Ricardo Silva Jacinto<sup>8</sup>, Sophie Hage<sup>9</sup> , Martin Hasenhüttl<sup>10,11</sup> , Steve M. Simmons<sup>12</sup> , Catharina J. Heerema<sup>2,13</sup> , Maarten S. Heijnen<sup>5,14</sup>, Pascal Kunath<sup>4</sup>, Matthieu J. B. Cartigny<sup>1</sup> , Claire McGhee<sup>15</sup>, and Daniel R. Parsons<sup>16</sup>



Baker et al., GRL (2024)

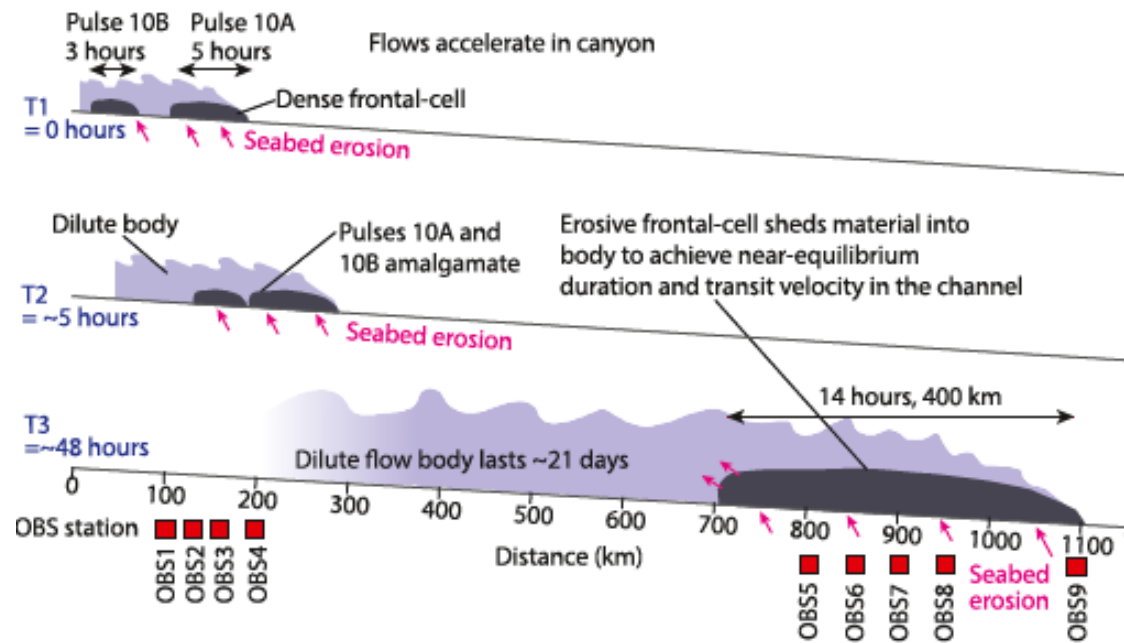


# Tracking turbidity currents



- Uniform velocity flow
- Increasing pulse duration
- Seabed erosion in « travelling wave » model

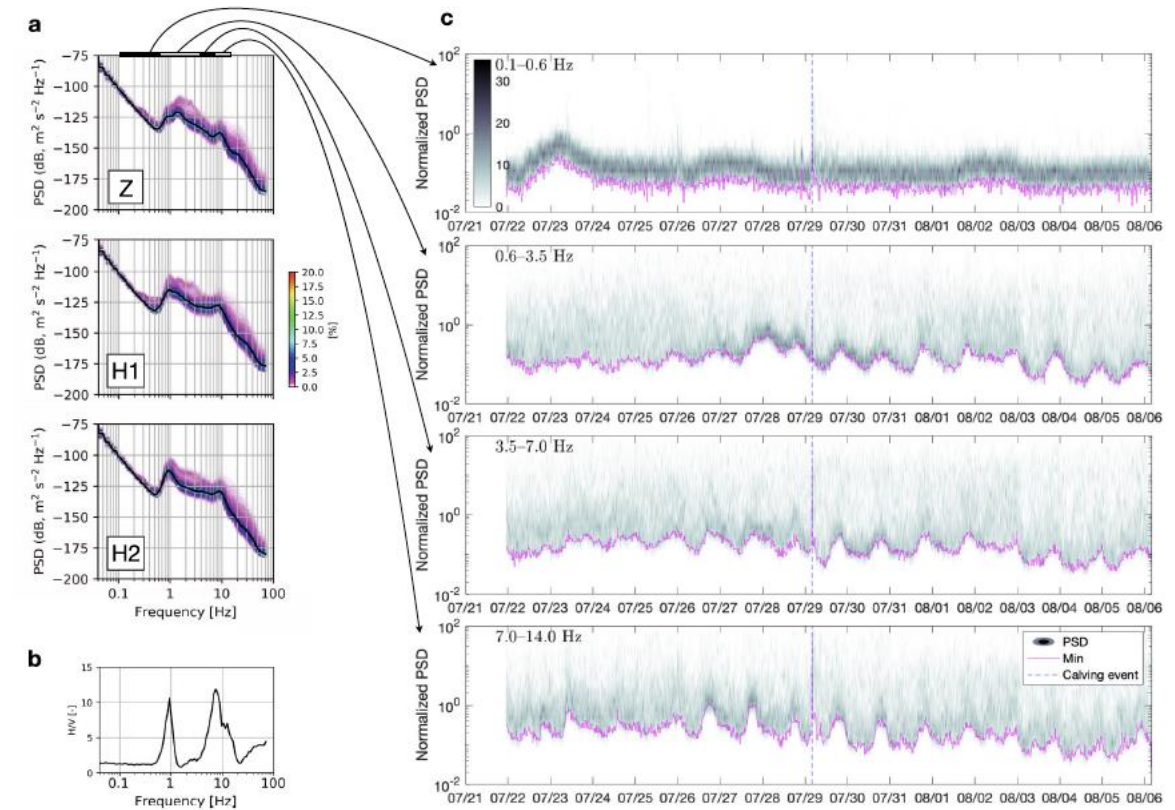
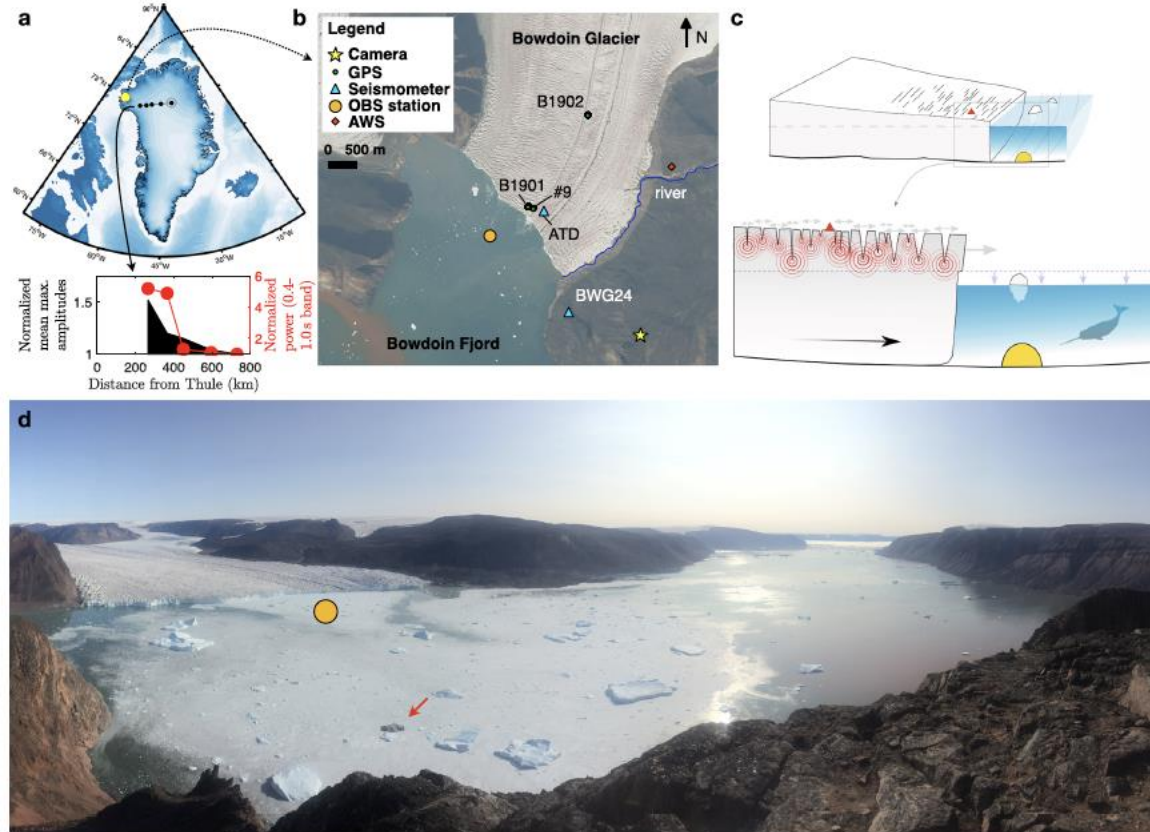
d) Observations of >1000 km runout canyon-flushing turbidity currents in the Congo Canyon-Channel



# Tracking ice sheets and calving events

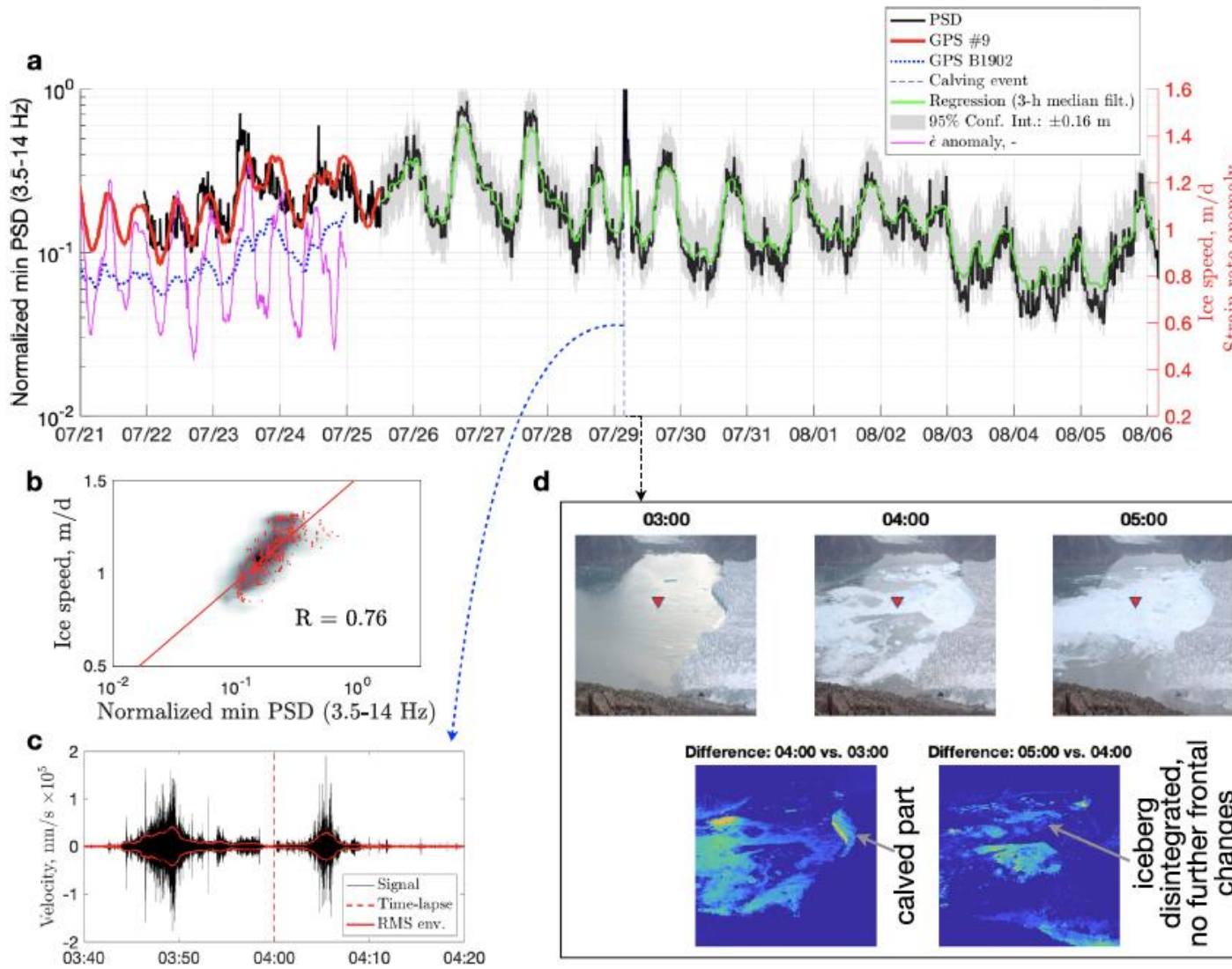
Ocean-bottom and surface seismometers reveal continuous glacial tremor and slip

Evgeny A. Podolskiy<sup>1,2</sup>✉, Yoshio Murai<sup>1,3</sup>, Naoya Kanna<sup>1,4</sup> & Shin Sugiyama<sup>1,2,5</sup>



- Single OBS near ice sheet front insulated from surface noise
- H/V shown at different frequencies

# Tracking ice sheets and calving events

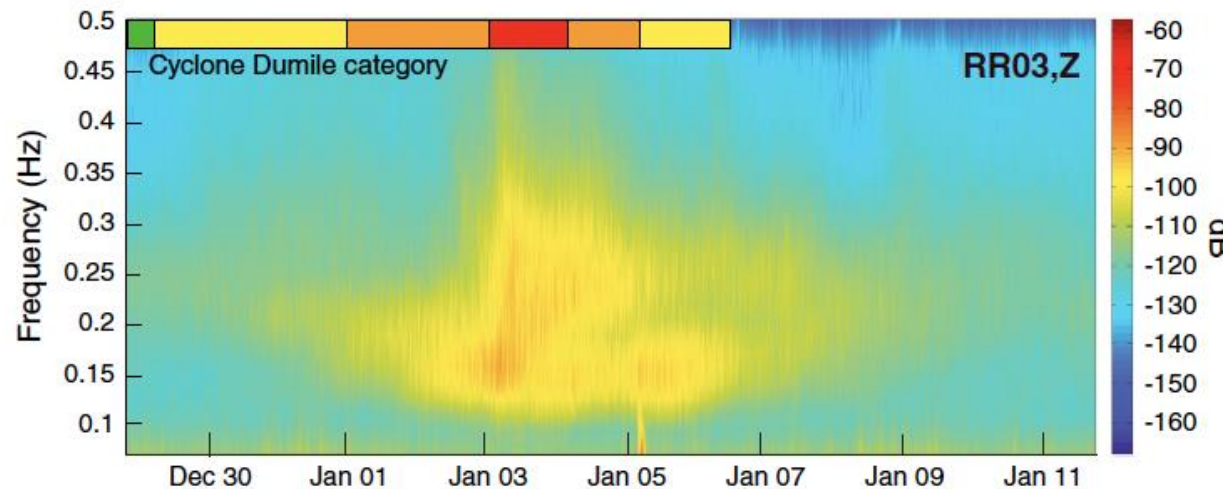


- Minimum PSD amplitude at 3.5-14 Hz tracks ice-speed observed from GNSS
- Regression can be used to monitor ice speed from a protected under-ice site
- During a calving event, OBS signals resemble tremors observed at tectonic plate boundaries (i.e., low-amplitude, long-duration, low-frequency, no clear phase onset).

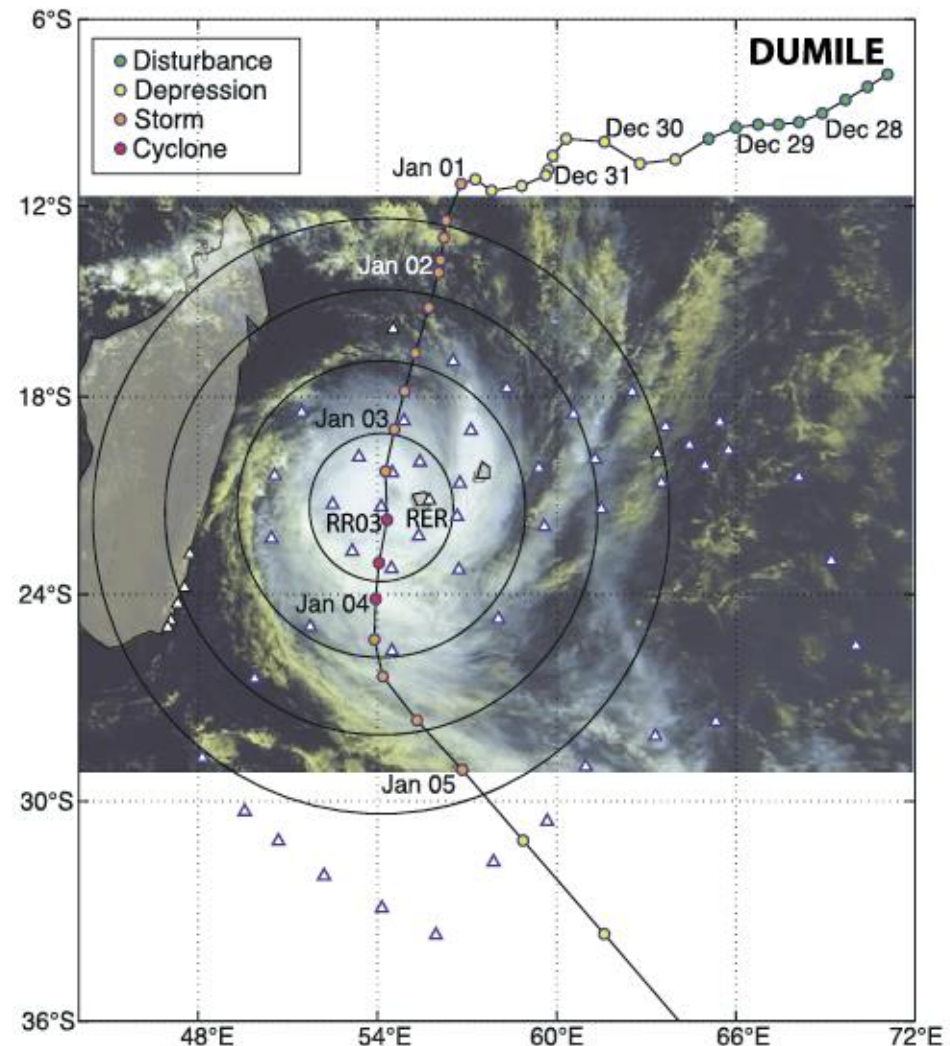
# Tracking storms from the seafloor

Tracking major storms from microseismic  
and hydroacoustic observations  
on the seafloor

Céline Davy<sup>1</sup>, Guilhem Barruol<sup>1</sup>, Fabrice R. Fontaine<sup>1</sup>, Karin Sigloch<sup>2,3</sup>, and Eléonore Stutzmann<sup>4</sup>

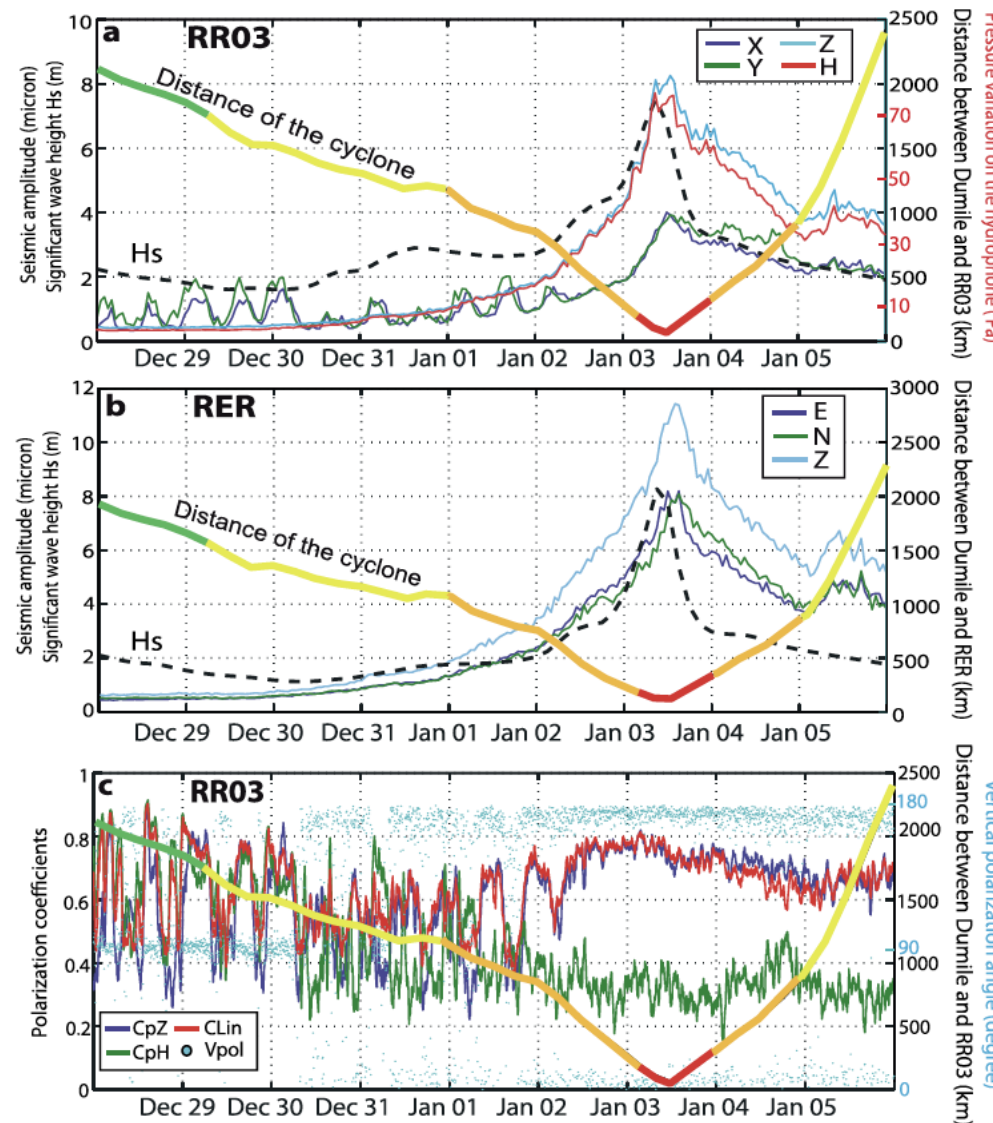


- Spectrogram shows the change in amplitude and frequency of microseismicity with time from the storm's evolution (disturbance to cyclone).

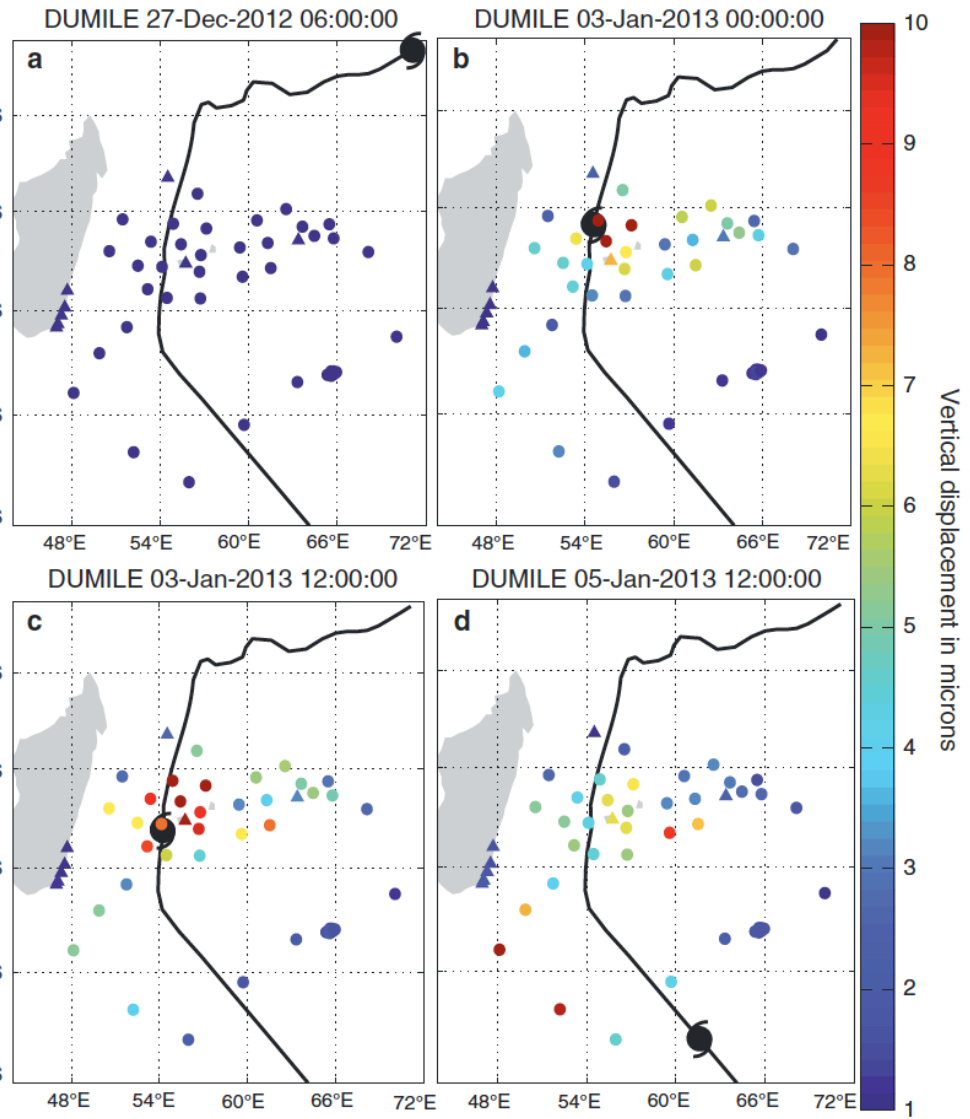


# Tracking storms from the seafloor

OBS



Land station

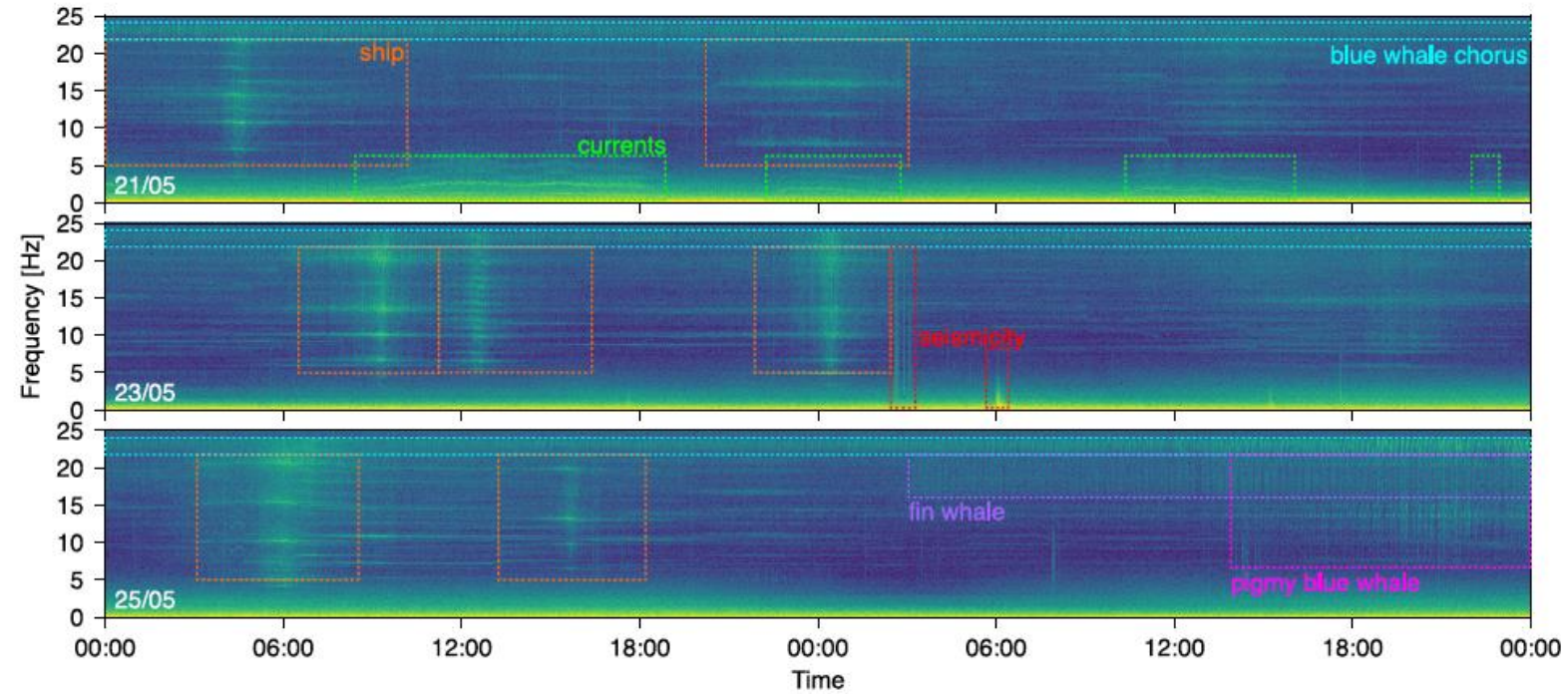
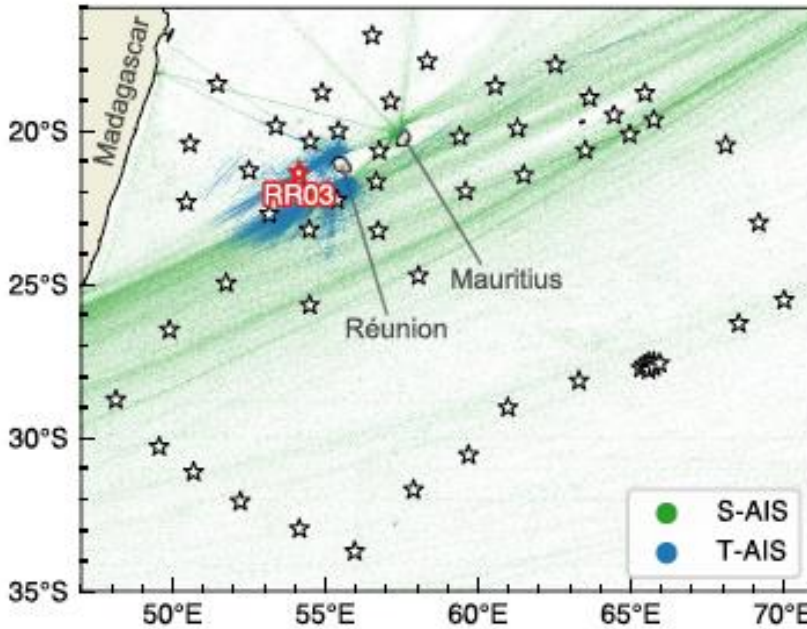


OBS polarization

# Ship detection and tracking

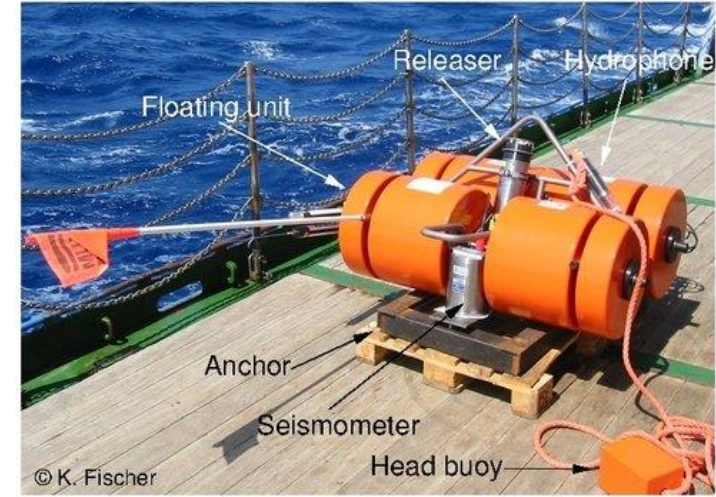
## Ship detection and tracking from single ocean-bottom seismic and hydroacoustic stations

Alister Trabattoni,<sup>1,a,b</sup>  Guilhem Barruol,<sup>1,c</sup>  Richard Dréo,<sup>1,b</sup>  and Abdel Boudraa<sup>2</sup> 

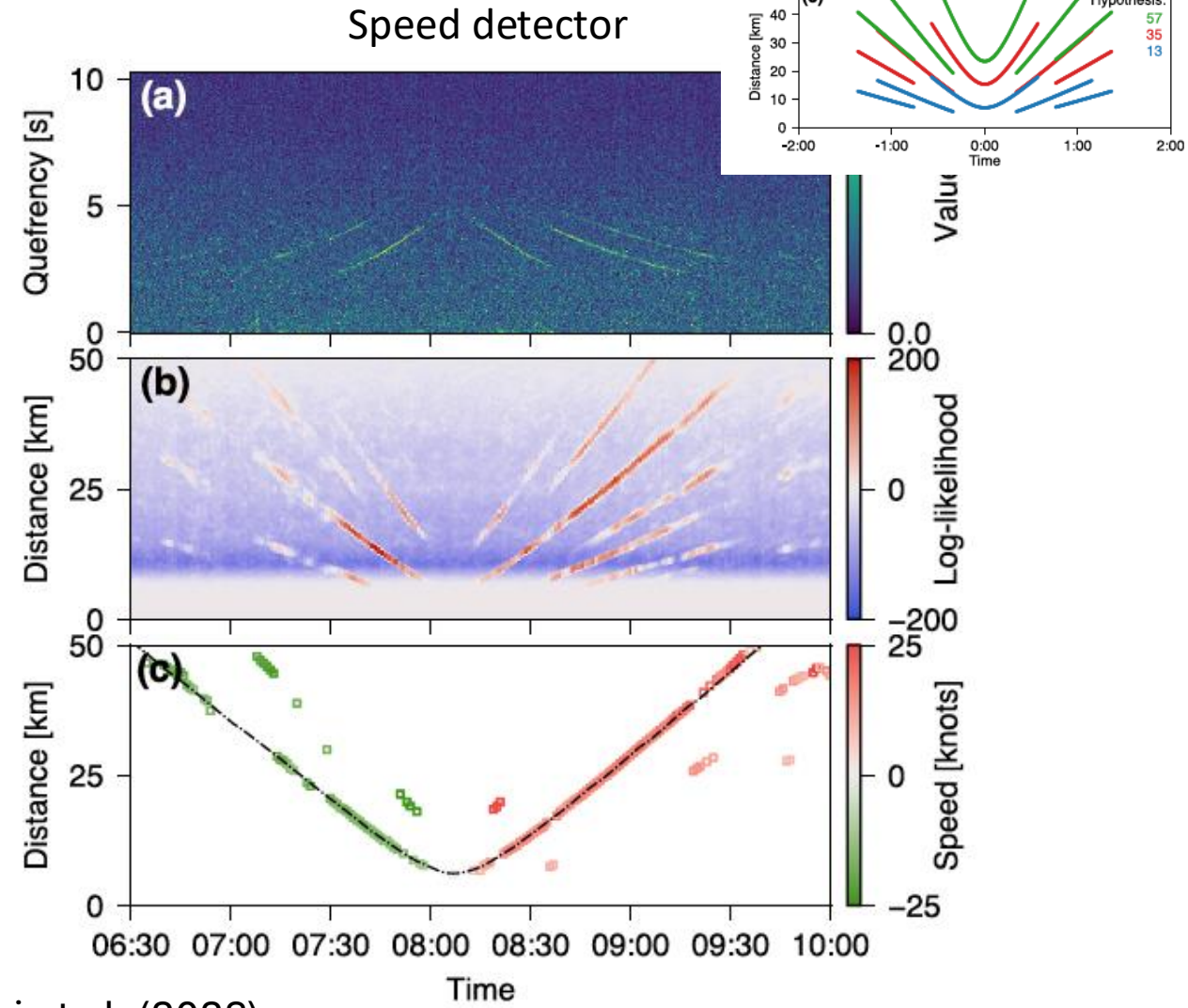
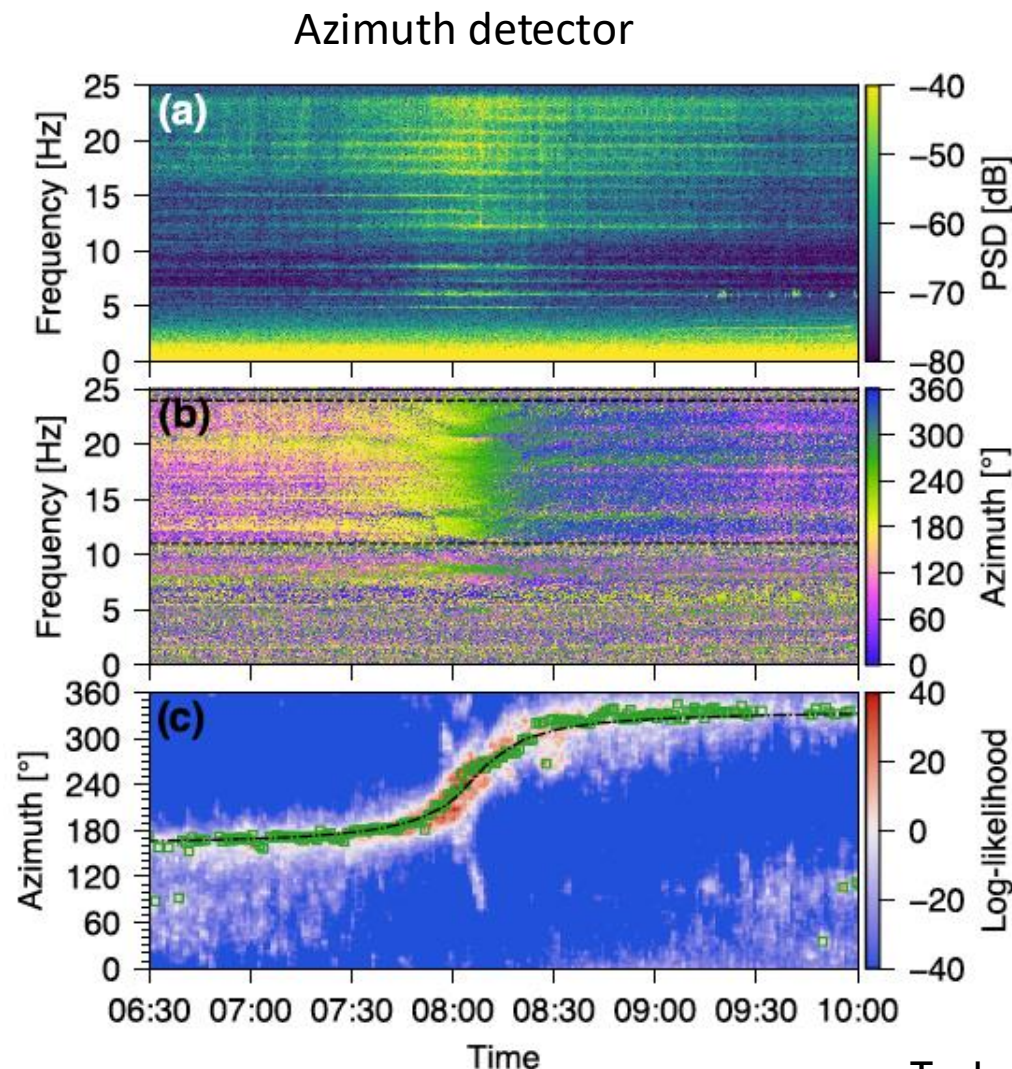


AIS: Automatic identification System  
S/T: Satellite or Terrestrial

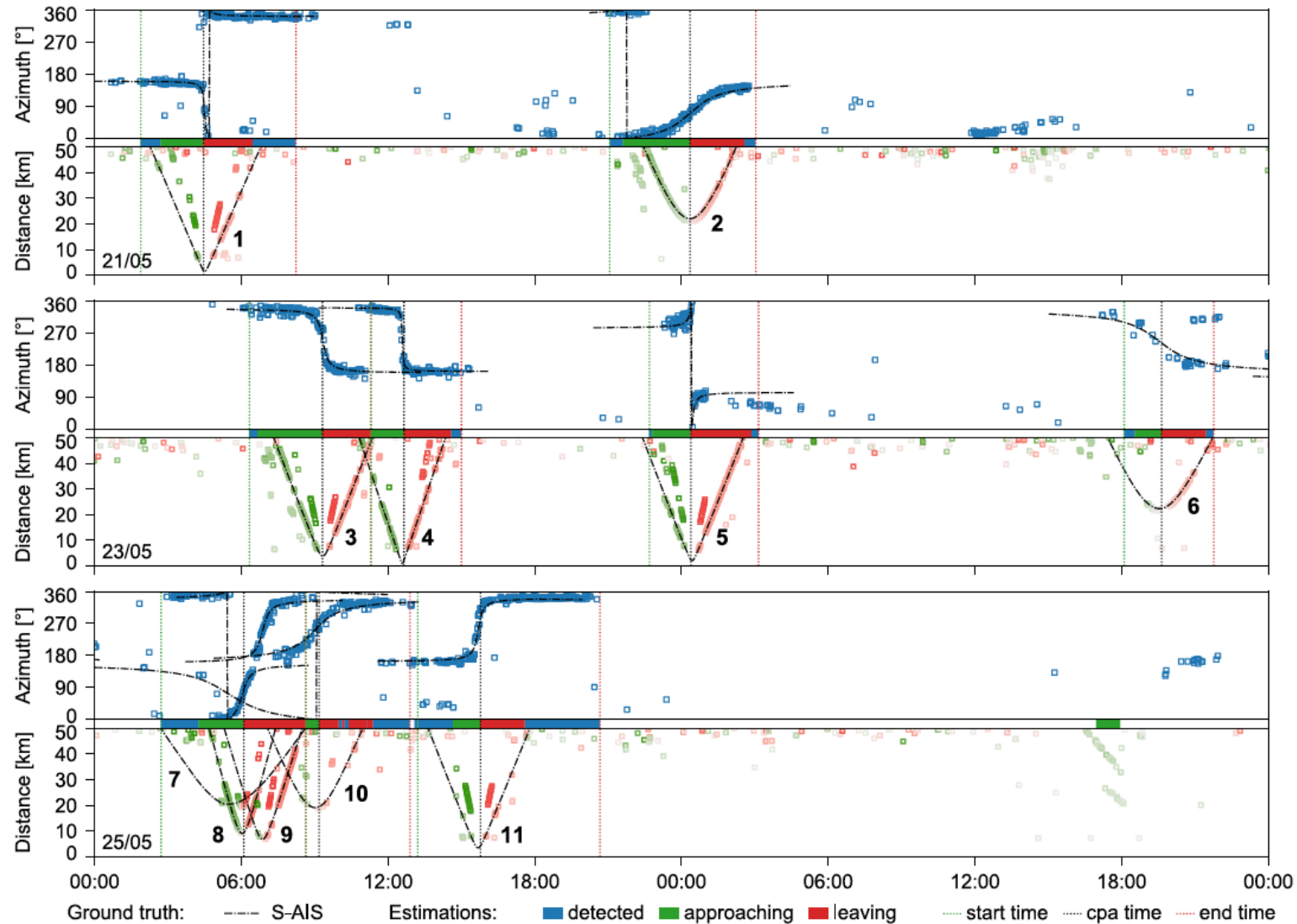
6-day soundscape: ships, whales, currents and earthquakes!



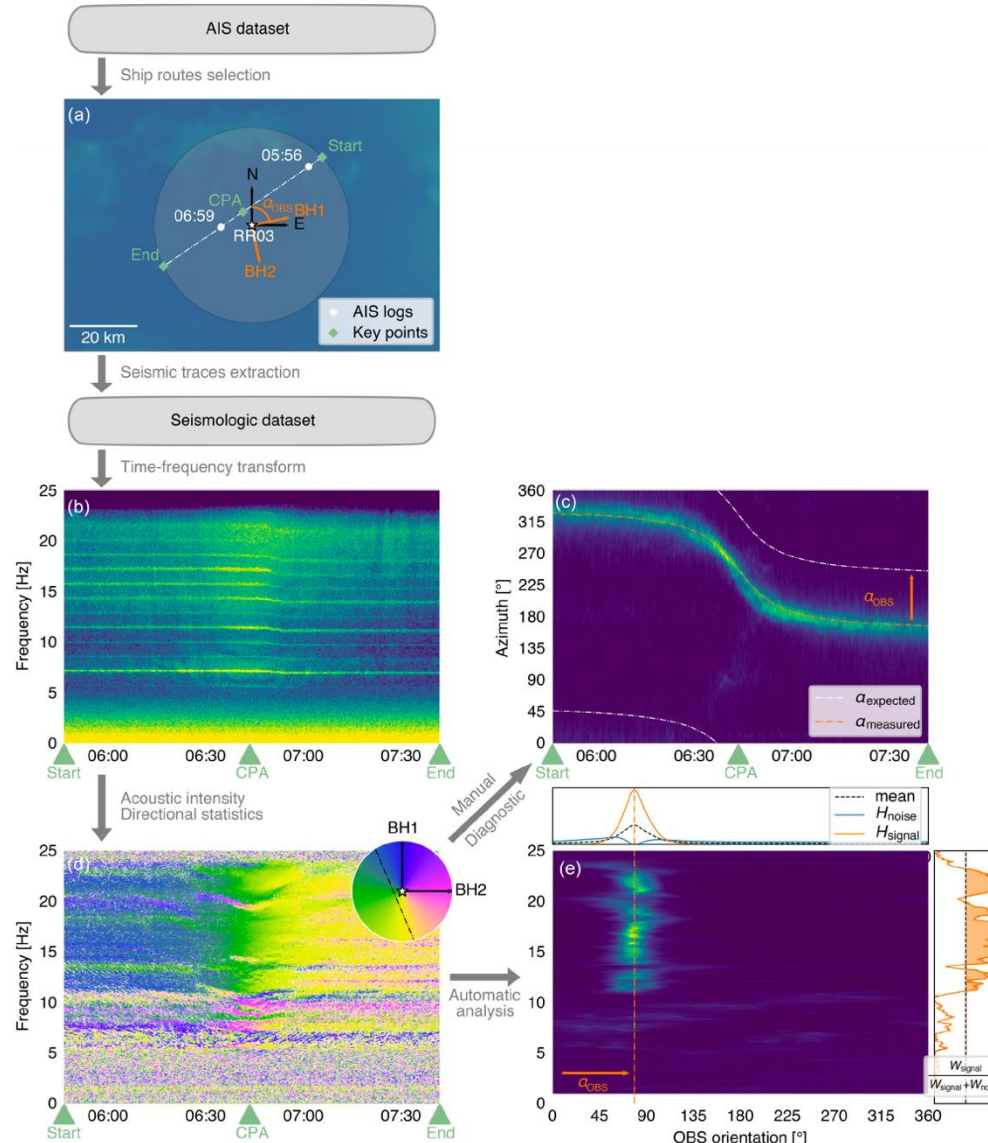
# Tracking ship direction and speed



# Tracking ship direction and speed

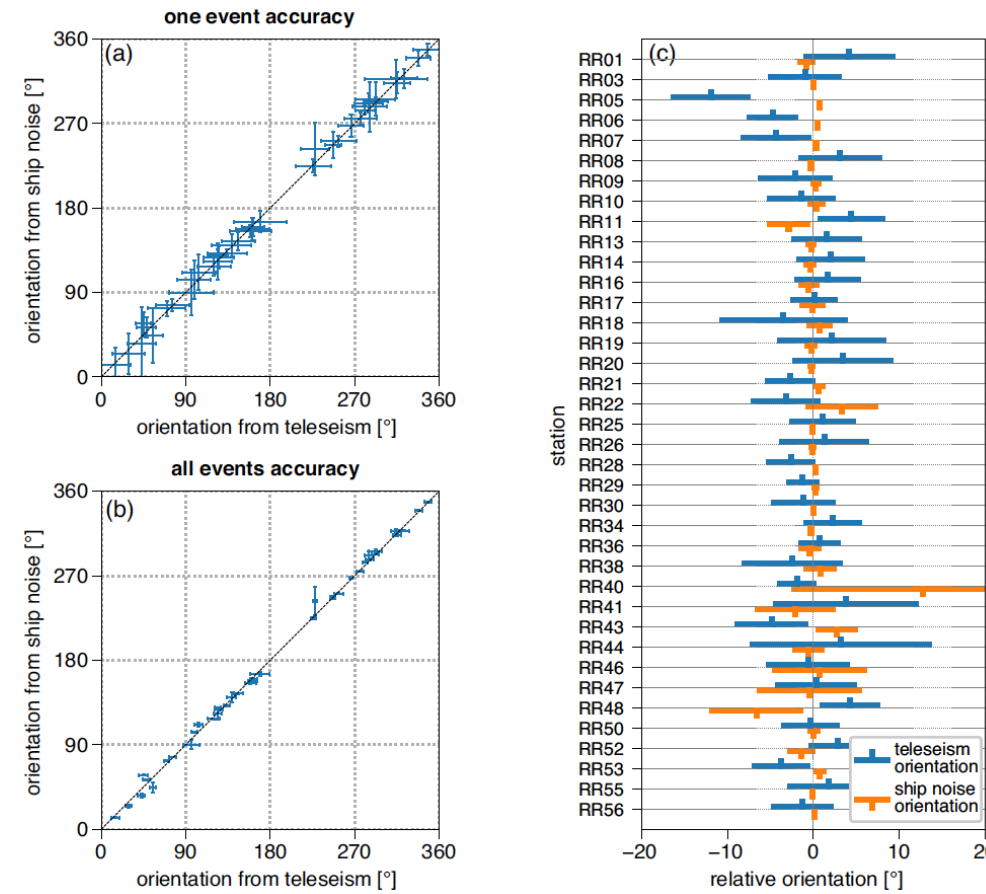


# OBS orientation from ship noise



Orienting and locating ocean-bottom seismometers from ship noise analysis

A. Trabattoni<sup>D, 1</sup>, G. Barruol<sup>D, 1</sup>, R. Dreö<sup>D, 2</sup>, A.O. Boudraa<sup>D, 2</sup> and F.R. Fontaine<sup>D, 1,3</sup>



# Summary

Seafloor noise contains many sources:

- Micro-seismic noise (wave-solid Earth interactions; mix of compressional and surface waves):  $T = 5\text{-}20$  seconds
- Compliance noise (infragravity waves): depth-dependent;  $T > 10\text{-}50$  secs
- Tilt noise:  $T > 10$  secs
- Whale vocalizations:  $\sim 5$  to  $> 100$  Hz
- Storms: micro-seismic peak
- Ships: 5 – 50 Hz

Visualization using spectrograms is the key!

# References

- Megan L. Baker, Sophie Hage, Peter J. Talling, Sanem Acikalin, Robert G. Hilton, Negar Haghipour, Sean C. Ruffell, Ed L. Pope, Ricardo Silva Jacinto, Michael A. Clare, Sefa Sahin; Globally significant mass of terrestrial organic carbon efficiently transported by canyon-flushing turbidity currents. *Geology* 2024; 52 (8): 631–636. doi: <https://doi.org/10.1130/G51976.1>
- Baker, M. L., Talling, P. J., Burnett, R., Pope, E. L., Ruffell, S. C., Urlaub, M., et al. (2024). Seabed seismographs reveal duration and structure of longest runout sediment flows on Earth. *Geophysical Research Letters*, 51, e2024GL111078. <https://doi.org/10.1029/2024GL111078>
- Davy, C., G. Barruol, F. R. Fontaine, K. Sigloch, and E. Stutzmann (2014), Tracking major storms from microseismic and hydroacoustic observations on the seafloor, *Geophys. Res. Lett.*, 41, 8825–8831, doi:10.1002/2014GL062319.
- Crawford, W. C., Webb, S. C., & Hildebrand, J. A. (1991). Seafloor compliance observed by long-period pressure and displacement measurements. *Journal of Geophysical Research: Solid Earth*, 96(B10), 16151-16160. <https://doi.org/10.1029/91JB01577>
- Wayne C. Crawford, Spahr C. Webb; Identifying and Removing Tilt Noise from Low-Frequency (<0.1 Hz) Seafloor Vertical Seismic Data. *Bulletin of the Seismological Society of America* 2000;; 90 (4): 952–963. doi: <https://doi.org/10.1785/0119990121>
- Janiszewski, H. A., Gaherty, J. B., Abers, G. A., Gao, H., & Eilon, Z. C. (2019). Amphibious surface-wave phase-velocity measurements of the Cascadia subduction zone. *Geophysical Journal International*, 217(3), 1929-1948. <https://doi.org/10.1093/gji/ggz051>
- Kent et al., Passive acoustic monitoring of baleen whales in Geographe Bay, Western Australia, *Acoustics Australia*, 2012: [https://www.researchgate.net/publication/249278667\\_Passive\\_acoustic\\_monitoring\\_of\\_baleen\\_whales\\_in\\_Geographe\\_Bay\\_Western\\_Australia](https://www.researchgate.net/publication/249278667_Passive_acoustic_monitoring_of_baleen_whales_in_Geographe_Bay_Western_Australia)

- Podolskiy, E. A., Murai, Y., Kanna, N., & Sugiyama, S. (2021). Ocean-bottom and surface seismometers reveal continuous glacial tremor and slip. *Nature Communications*, 12(1), 1-11. <https://doi.org/10.1038/s41467-021-24142-4>
- Schwardt, M., Pilger, C., Gaebler, P. et al. Natural and Anthropogenic Sources of Seismic, Hydroacoustic, and Infrasonic Waves: Waveforms and Spectral Characteristics (and Their Applicability for Sensor Calibration). *Surv Geophys* 43, 1265–1361 (2022). <https://doi.org/10.1007/s10712-022-09713-4>.
- Stephen, R. A., F. N. Spiess, J. A. Collins, J. A. Hildebrand, J. A. Orcutt, K. R. Peal, F. L. Vernon, and F. B. Wooding (2003), Ocean Seismic Network Pilot Experiment, *Geochem. Geophys. Geosyst.*, 4, 1092, doi:10.1029/2002GC000485, 10.
- Jean Baptiste Tary, Christine Peirce, Richard W. Hobbs, Felipe Bonilla Walker, Camilo De La Hoz, Anna Bird, Carlos Alberto Vargas; Application of a seismic network to baleen whale call detection and localization in the Panama basin—a Bryde's whale example. *J. Acoust. Soc. Am.* 1 March 2024; 155 (3): 2075–2086. <https://doi.org/10.1121/10.0025290>
- Trabattoni, A., Barruol, G., Dreö, R., Boudraa, A. O., & Fontaine, F. R. (2020). Orienting and locating ocean-bottom seismometers from ship noise analysis. *Geophysical Journal International*, 220(3), 1774-1790. <https://doi.org/10.1093/gji/ggz519>
- Alister Trabattoni, Guilhem Barruol, Richard Dréo, Abdel Boudraa; Ship detection and tracking from single ocean-bottom seismic and hydroacoustic stations. *J. Acoust. Soc. Am.* 1 January 2023; 153 (1): 260–273. <https://doi.org/10.1121/10.0016810>
- Webb, S. C. (1998), Broadband seismology and noise under the ocean, *Rev. Geophys.*, 36(1), 105–142, doi:10.1029/97RG02287.
- Weirathmueller, M. J., Stafford, K. M., D. Wilcock, W. S., Hilmo, R. S., Dziak, R. P., & Tréhu, A. M. (2017). Spatial and temporal trends in fin whale vocalizations recorded in the NE Pacific Ocean between 2003-2013. *PLOS ONE*, 12(10), e0186127. <https://doi.org/10.1371/journal.pone.0186127>.